ADVANCED RESEARCH PROJECTS AGENCY

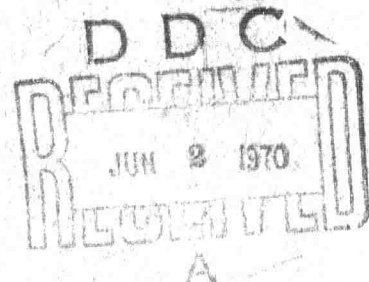Contract ARPA SD-88

Technical Report No. ARPA-40

NECKING IN A BAR

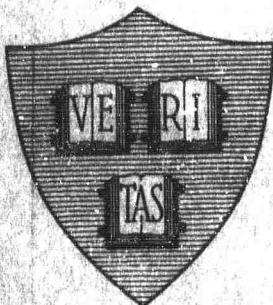March 1970

By

Winston H. Chen

DIVISION OF ENGINEERING AND APPLIED PHYSICS
HARVARD UNIVERSITY · CAMBRIDGE, MASSACHUSETTS

DISCLAIMER NOTICE

THIS DOCUMENT IS THE BEST
QUALITY AVAILABLE.

COPY FURNISHED CONTAINED
A SIGNIFICANT NUMBER OF
PAGES WHICH DO NOT
REPRODUCE LEGIBLY.

NECKING IN A BAR

By

Winston H. Chen

Technical Report No. ARPA-40

Contract ARPA SD-88

March 1970

Submitted to:

Advanced Research Projects Agency

The Department of Defense

Division of Engineering and Applied Physics

Harvard University

Cambridge, Massachusetts

NECKING IN A BAR

By

Winston H. Chen

Division of Engineering and Applied Physics

Harvard University · Cambridge, Massachusetts

ABSTRACT

The necking process of an axisymmetric tension specimen made of elastic-plastic, strain-hardening material is analyzed by a generalized J_2-flow theory for large deformations. The governing equations are solved in a Kantorovich type approach based on a variational principle. The effects of both geometric nonlinearities resulting from large deformations and the physical nonlinearities arising from plastic material behavior are considered. Numerical results have been found for the stress and deformation histories in the specimen up to a 50% reduction of the neck radius. The shape of the neck, for the first time, is rationally calculated.

TABLE OF CONTENTS

BLANK PAGE

I. Introduction

The conventional tension test is usually considered to provide the basic tensile properties of materials. The test does provide knowledge of the intrinsic stress-strain relation up to a point. However, after necking occurs in a tension specimen, the distributions of stress and strain become very complicated and are not known. The information obtainable from the test thereafter is only some kind of average stress-average strain relation. A typical tension specimen after necking occurs is shown schematically in Fig. 1.

In order to provide a better understanding of the true stress-strain relation, Bridgman [1] studied the stress distribution at the narrowest section (section A-B in Fig. 1) of a necked-down axisymmetric tension specimen and obtained a semi-empirical solution. His analysis was based on the assumption that the axial strain across the narrowest section was uniform. Davidenkov and Spiridonova [2], by an analysis similar to Bridgman's, obtained another result for the stress distribution at the neck. In both of these analyses the displacements and hence the shapes of the necked profiles of the tension specimen were not calculated. In fact, the determination of the stress distribution had to rely on measured values of the neck diameter d and radius of curvature ρ (see Fig. 1). These solutions, therefore, were not entirely rational. Thomason [3] has calculated the profiles of the axisymmetrically necking tension specimen, based on a "maximum unloading rate" hypothesis. But no solution for the stress distribution was included in his analysis. Recently, Segal [4] has studied the plastic flow in the neighborhood of the neck of an ideally plastic tension specimen. He made some calculations both for the stress and the displacement fields. However, the analysis did not provide
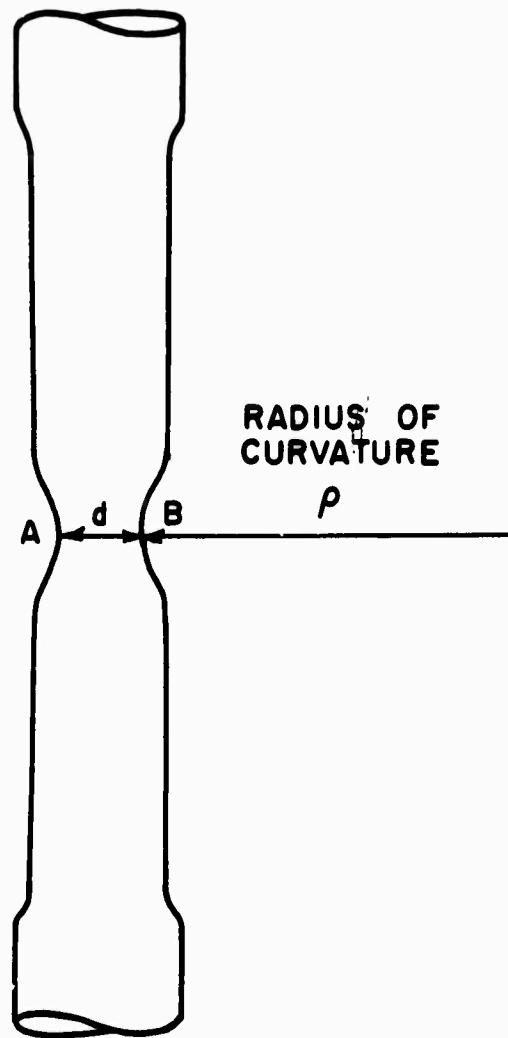
-1-

FIG 1 NECKED-DOWN TENSION SPECIMEN

a complete solution for the stress and the strain distributions. These earlier investigations evidently do not provide an adequate analytical solution to the problem of necking in strain-hardening bars.

In a rigorous analysis, it is necessary to find the displacement and the stress in the whole specimen, not just at the neck; and for the complete loading history, not just at a particular deformation stage. The effects of plastic unloading must be considered; also, the large changes in geometry that occur during necking must be taken into account.

The purpose of the present analysis is to calculate rationally the deformation (and hence the necking shape) and the stress distribution in a tension specimen throughout its loading history. The tension speci-men considered is of finite length and initially has some imperfection on the lateral surfaces in such a way that the radius at the middle is slightly smaller than the radius at the ends. The specimen is subjected to a uniform axial displacement at the ends and is elongated in such a way that the ends remain shear free. The specimen material is assumed to be isotropic, elastic-plastic, and strain-hardening. A variational equation of equilibrium for large deformation, in conjunction with the approximation method due to Kantorovich [5], is used to solve for the field variables. A generalized J_2-flow theory for elastic-plastic materials with large deformation effects is used in the analysis. Thus, both the effects of the geometric nonlinearities resulting from large deformations and the physical nonlinearities arising from plastic material behavior are included in this analysis.

II. Field Equations

A set of field equations for analyzing arbitrary deformations of elastic-plastic materials will be presented. The equations involved are written in a general form with the use of tensor notation.

2.1. Equilibrium

The notation and equations of equilibrium used in the present analysis follow those of [6]. The pertinent results of [6] will be briefly reviewed.

Let a material point of a solid body be identified by the coordinates (ξ^1, ξ^2, ξ^3) and let the vectors $\underline{r}$ and $\underline{\bar{r}}$ denote respecitvely, its position when the body is undeformed and deformed. The covariant base vectors of the undeformed and deformed body are $\underline{e}_i = \dfrac{\partial \underline{r}}{\partial \xi^i}$, and $\underline{\bar{e}}_i = \dfrac{\partial \underline{\bar{r}}}{\partial \xi^i}$. respectively, and the covariant components of the metric tensors are

$$g_{ij} = \underline{e}_i \cdot \underline{e}_j$$

$$G_{ij} = \underline{\bar{e}}_i \cdot \underline{\bar{e}}_j$$

with inverses g^{ij} and G^{ij}. The contravariant base vectors are $\underline{e}^i = g^{ij}\underline{e}_j$ and $\underline{\bar{e}}^i = G^{ij}\underline{\bar{e}}_j$.

One defines the contravariant tensor components u^i of displacement $\underline{u} = \underline{\bar{r}} - \underline{r}$ by the relation

$$\underline{u} = u^i \underline{e}_i \quad . \tag{1}$$

The Lagrangian strain tensor is defined by

$$\eta_{ij} = \frac{1}{2}(G_{ij} - g_{ij}) = \frac{1}{2}(\nabla_j u_i + \nabla_i u_j) + \frac{1}{2}g_{st}(\nabla_i u^s)(\nabla_j u^t) \tag{2}$$

where ∇_i denotes covariant differentiation in the undeformed body. The stress tensor $\underline{\sigma}$ in the deformed body may be written symbolically in terms of its contravariant components σ^{ij} as

$$\underline{\sigma} = \sigma^{ij}\underline{\bar{e}}_i\underline{\bar{e}}_j \quad . \tag{3}$$

Consider an arbitrary volume V of the undeformed body bounded by a surface S; after deformation these become $\overline{V}$ and $\overline{S}$, respectively. Let $\underset{\sim}{n}$ be the unit normal to S and define n_i by the relation

$$\underset{\sim}{n} = n_i \underset{\sim}{e}^i \quad .$$

If body forces are neglected, the equation of force equilibrium governing the stress rate and displacement rate given in [6] is

$$\nabla_i (\dot{q}^{ir} + \dot{q}^{ij}\nabla_j u^r + q^{ij}\nabla_j \dot{u}^r) = 0 \tag{4}$$

where $q^{ij} = \dfrac{\overline{G}}{g}\,\sigma^{ij}$ is the Kirchhoff stress; here G and g are the determinants of G_{ij} and g_{ij}, respectively, and where ($\cdot$) denote differentiation with respect to a monotonically increasing quantity such as time t.

If surface traction rates $\underset{\sim}{\dot{T}} = \dot{T}^i \underset{\sim}{e}_i$ per unit original area are prescribed, then

$$(\dot{q}^{ir} + \dot{q}^{ij}\nabla_j u^r + q^{ij}\nabla_j \dot{u}^r)n_i = \dot{T}^r \tag{5}$$

on the boundary. Prescribed displacement rates $\underset{\sim}{\dot{v}} = \dot{v}^i \underset{\sim}{e}_i$ are satisfied by letting $\dot{u}^i = \dot{v}_i$.

A variational equation governing $\dot{u}^i$ and $\dot{q}^{ij}$, which can be deduced from the classical principle of virtual work, is

$$\int_V \{\dot{q}^{ij}\delta\dot{\eta}_{ij} + \tfrac{1}{2}q^{ij}\delta[g_{st}(\nabla_i \dot{u}^s)(\nabla_j \dot{u}^t)]\}dV = \int_S \dot{T}^i \delta\dot{u}_i \, dS \tag{6}$$

for all states $\dot{q}^{ij}$, $\dot{u}^i$, $\dot{T}^i$ satisfying equilibrium, and all displacement variations $\delta\dot{u}_i$, with

$$\delta\dot{\eta}_{ij} = \tfrac{1}{2}\{[\nabla_j \delta\dot{u}_i + \nabla_i \delta\dot{u}_j] + g_{st}[(\nabla_i u^s)(\nabla_j \delta\dot{u}^t) + (\nabla_j u^t)(\nabla_i \delta\dot{u}^s)]\} \quad .$$

Either the equilibrium equation (4) or the variational equation of equilibrium (6) can be used, in principle, for analyzing plasticity problems

involving large deformations. In the present analysis, the variational equation (6) will be used, in conjunction with a Kantorovich approximation method, to solve for the field variables.

he field equations are still incomplete and must be augmented by constitutive relations between stress and strain--or, more precisely, between stress rates and strain rates.

2.2. Constitutive Equation

There have been several forms of the constitutive equations for elastic-plastic materials involving large deformations, such as those suggested by Green and Naghdi [7], Lee and Liu [8], Cameron and Scorgie [9], Lee [10], and Willis [11]. However, in the present analysis of the large deformation in a tension specimen, the new constitutive equation given below seems to be more convenient to use.

The materials considered are isotropic, elastic-plastic and strain-hardening. For simplicity, neither a Bauschinger effect nor the influence of temperature is included. It is assumed that the actual strain rate $\dot{\eta}_{ij}$ can be written as the sum of the elastic strain rate $\dot{\eta}_{ij}^E$ and the plastic strain rate $\dot{\eta}_{ij}^P$. The elastic stress-strain relation as suggested by Budiansky [12] is

$$\dot{\eta}_{ij}^E = \frac{1}{E}\{\frac{1}{2}(1 + v)[G_{ik}\frac{d}{dt}(\sigma_j^k) + G_{jk}\frac{d}{dt}(\sigma_i^k)] - vG_{ij}\frac{d}{dt}(\sigma_k^k)\} \qquad (7)$$

where $\sigma_j^i = \sigma^{ik}G_{kj}$ is the mixed tensor component of the stress tensor, E is Young's modulus and v denotes Poisson's ratio. This is a generalized Hooke's law which includes large deformation effects. Equation (7) is not integrable and is not a rigorous constitutive relation derived from the theory of elasticity for arbitrary deformation. But it will not result in significant errors for the present analysis, because for infinitesimal

strain Equation (7) is the exact statement of Hooke's law; and for large deformation in the present necking problem, the elastic strain only plays a minor role and is dominated by the plastic strain.

The plastic stress-strain relation is a generalization of the J_2 flow theory to include large deformation effects. Let us begin with the J_2 flow theory for infinitesimal strains. Referred to the Cartesian coordinates, the stress and strain tensor components are σ_{ij} and ϵ_{ij}, the stress deviator is $s_{ij} = \sigma_{ij} - \frac{1}{3}\delta_{ij}\sigma_{kk}$, and the effective stress is defined by $\sigma_e = [\frac{3}{2}s_{ij}s_{ij}]^{\frac{1}{2}}$. The yield function is $F = \sigma_e - c$, where c is the initial yield stress or the maximum value of σ_e which has occurred in the stress history, and the flow rule states that the plastic strain rate is

$$\dot{\epsilon}_{ij}^p = \frac{3}{2}(\frac{1}{E_t} - \frac{1}{E})\frac{\dot{\sigma}_e}{\sigma_e}s_{ij} \quad \text{if} \quad \sigma_e = c \text{ and } \dot{\sigma}_e \equiv \frac{d}{dt}(\sigma_e) \neq 0$$

$$\dot{\epsilon}_{ij}^p = 0 \qquad \text{if} \quad \sigma_e < c,$$

$$\text{or } \sigma_e = c \text{ and } \dot{\sigma}_e \leq 0$$

where E_t is the tangent modulus, which is the slope of the uniaxial stress-strain curve.

Next, let large deformation effects be included. Referred to general coordinates, the contravariant components of stress are σ^{ij}, and the contravariant components of the stress deviator tensor $\underset{\sim}{s}$ are

$$s^{ij} = \sigma^{ij} - \frac{1}{3}G^{ij}\sigma^{kl}G_{kl} \quad .$$

The mixed tensor components s_j^i are defined as

$$s_j^i = \sigma_j^i - \frac{1}{3}\delta_j^i\sigma^{kl}G_{kl}$$

where δ^i_j $G^{ik}G_{k}$ is the Kronecker delta and $\sigma^{kl}G_{kl}$ is the mean normal stress. The effective stress is

$$\sigma_e \quad (\tfrac{3}{2}s^i_j s^j_i)^{\frac{1}{2}}$$

$$[\tfrac{3}{2}(\sigma^{ij}\sigma^{kl}G_{ik}G_{jl} - \tfrac{1}{3}\sigma^{ij}\sigma^{kl}G_{ij}G_{kl})]^{\frac{1}{2}} \quad . \tag{8}$$

and the yield function is still $F - \sigma_e - c$. The generalized flow rule states that

$$\dot{\eta}^P_{ij} \quad \tfrac{3}{2}(\tfrac{1}{E_t} - \tfrac{1}{E})(\sigma^{kl}G_{ki}G_{lj} - \tfrac{1}{3}G_{ij}\sigma^{kl}G_{kl})\frac{\dot{\sigma}_e}{\sigma_e} \text{ if } \sigma_e - c \text{ and } \dot{\sigma}_e \ge 0$$

$$\tag{9a}$$

$$\dot{\eta}^P_{ij} - 0 \qquad\qquad \text{if} \quad \sigma_e < c .$$

$$\text{or} \quad \sigma_e - c \text{ and } \dot{\sigma}_e \le 0 \tag{9b}$$

where, as shown later, the tangent modulus E_t is now defined as the slope of the true stress-natural strain curve in uniaxial tension. Note that the plastic strain given by (9)a satisfies the plastic incompressibility condition. This can be seen by examining the rate of change of volume which is

$$\frac{d}{dt}(d\overline{V}) \cdot \frac{d}{dt}(\cdot \frac{G}{g} dV) \cdot \frac{1}{2} \cdot \frac{\overline{G}}{g} G^{ij}\dot{G}_{ij}dV$$

$$\cdot \frac{\overline{G}}{g} G^{ij}(\dot{\eta}^E_{ij} + \dot{\eta}^P_{ij})dV \quad .$$

The change of volume contributed by the plastic strain rate is $\cdot \frac{\overline{G}}{g} G^{ij}\dot{\eta}^P_{ij}dV$, which by (9)a, vanishes.

Combining equations (7) and (9) gives the full constitutive equation

$$\dot{\eta}_{ij} = \frac{1}{E}\left[\frac{1}{2}(1 + \nu)(G_{ik}\dot{\sigma}^k_j + G_{jk}\dot{\sigma}^k_i) - \nu G_{ij}\dot{\sigma}^k_k\right] \text{ if } \sigma_e = c \text{ and } \dot{\sigma}_e > 0$$

$$+ \frac{3}{2}(\frac{1}{E_t} - \frac{1}{E})(\sigma^{kl}G_{kl}G_{ij} - \frac{1}{3}G_{ij}\sigma^{kl}G_{kl})\frac{\dot{\sigma}_e}{\sigma_e} \qquad (10)a$$

$$\dot{\eta}_{ij} = \frac{1}{E}\left[\frac{1}{2}(1 + \nu)(G_{ik}\dot{\sigma}^k_j + G_{jk}\dot{\sigma}^k_i) - \nu G_{ij}\dot{\sigma}^k_k\right] \text{ if } \sigma_e < c,$$

$$\text{or } \sigma_e = c \text{ and } \dot{\sigma}_e < 0$$

$$(10)b$$

Physically, Equation (10)a applies in the plastic loading region and (10)b applies in the plastic unloading or elastic region. The strain rate given by (10)a depends not only on the current stress rates but also on the whole stress and deformation histories.

In order to define E_t precisely, let us now consider uniaxial tension. The stress-strain relation then reduces to

$$\dot{\eta}_{11} = \frac{1}{E}[G_{11}\dot{\sigma}^1_1] + [\frac{1}{E_t} - \frac{1}{E}]\sigma^{11}G_{11}G_{11}\frac{\dot{\sigma}_e}{\sigma_e} \text{ if } \sigma_e = c \text{ and } \dot{\sigma}_e > 0$$

$$(11)a$$

$$\dot{\eta}_{11} = \frac{1}{E}G_{11}\dot{\sigma}^1_1 \qquad \text{ if } \sigma_e < c,$$

$$\text{or } \sigma_e = c \text{ and } \dot{\sigma}_e < 0 \qquad (11)b$$

where the effective stress σ_e is $\sigma^{11}G_{11} = \sigma^1_1$, by Equation (8). Since σ^{11} is the tensor component referred to the base vector $\bar{g}_1$, which has the magnitude G_{11}, the corresponding physical component of stress is

$$\sigma_{xx} = \sigma^{11} \cdot G_{11} \cdot \overline{G_{11}} = \sigma^1_1 = \sigma_e$$

Therefore, Equations (11)a and (11)b become

$$\frac{\dot{\eta}_{11}}{G_{11}} = \frac{1}{E_t}\dot{\sigma}_{xx} \qquad (12)a$$

$$\frac{\dot{\eta}_{11}}{G_{11}} = \frac{1}{E}\dot{\sigma}_{xx} \quad . \tag{12}b$$

The natural strain is defined by

$$\bar{\eta} = \ln(\frac{\ell}{\ell_0}) = \ln(1 + \frac{\partial u_x}{\partial x}) = \frac{1}{2}\ln(1 + 2\eta_{11}) \tag{13}$$

where u_x is the displacement along the coordinate x; ℓ_0 and ℓ are the original and the current length of a cylindrical bar subjected to uniaxial tension. The rate of change of the natural strain is

$$\dot{\bar{\eta}} = \frac{\dot{\eta}_{11}}{1 + 2\eta_{11}} = \frac{\dot{\eta}_{11}}{G_{11}} \quad . \tag{14}$$

By comparing (12) and (14), we obtain the following simple relations for the uniaxial tension case:

$$\dot{\bar{\eta}} = \frac{1}{E_t}\dot{\sigma}_{xx} \qquad \text{if } \sigma_{xx} = c \text{ and } \dot{\sigma}_{xx} > 0$$

$$\dot{\bar{\eta}} = \frac{1}{E}\dot{\sigma}_{xx} \qquad \text{if } \sigma_{xx} < c,$$

$$\qquad \text{or } \sigma_{xx} = c \text{ and } \dot{\sigma}_{xx} \leq 0$$

Now the tangent modulus E_t is clearly seen to be the slope of the true stress-natural strain curve as shown in Fig. 2, and E is the linear relationship between $\bar{\eta}$ and σ_{xx} when plastic unloading occurs (as well as during loading in the absence of plastic flow). The constitutive equation (10) is used under the condition that the $\sigma_{xx} - \bar{\eta}$ relation (or equivalently E and E_t) in uniaxial tension is known.

The constitutive equation is complete, but its inversion (the stress rate in terms of the strain rates) is still to be found. This inversion must be used in conjunction with the variational equation (6), because
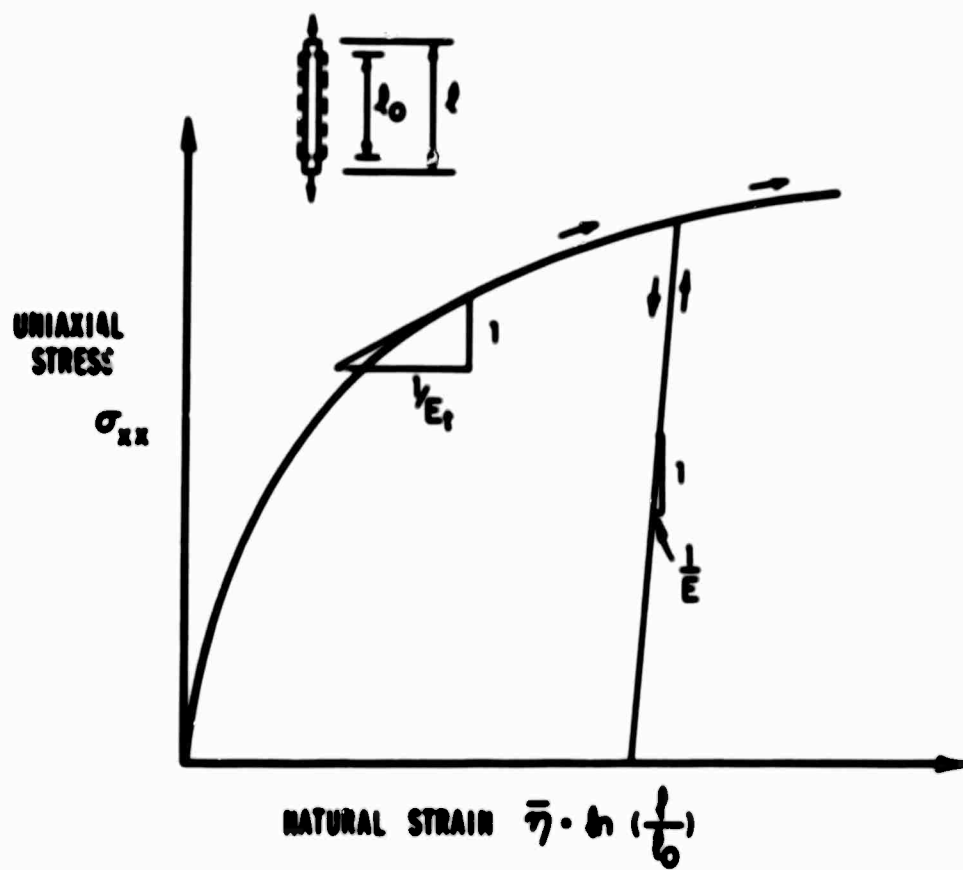
FIG. 2   UNIAXIAL   STRESS − STRAIN   RELATION

we wish to write σ^{ij} in terms of $\dot{\eta}_{ij}$, and successively write $\dot{\eta}_{ij}$ in terms of $\dot{u}^i$ and solve for $\dot{u}^i$. The inversion of (10) is derived in the Appendix; the result is

$$\sigma^{ij} = \frac{E}{(1+v)} \, G^{ik}G^{jl}\dot{\eta}_{kl} - \frac{3}{2} \frac{s^{ij}(\frac{1}{E_t} - \frac{1}{E})s^{kl}\dot{\eta}_{kl}}{\sigma_e^2(\frac{2}{3}\frac{(1+v)}{E} + (\frac{1}{E_t} - \frac{1}{E}))}$$

$$+ \frac{vE}{(1+v)(1-2v)} G^{ij}G^{kl}\dot{\eta}_{kl} - (\sigma^{ik}G^{jl}\dot{\eta}_{kl} + \sigma^{jk}G^{il}\dot{\eta}_{kl})$$

$$\text{if } \sigma_e = c \text{ and } s^{ij}\dot{\eta}_{ij} > 0 \qquad (15)a$$

$$\sigma^{ij} = \frac{E}{(1+v)} G^{ik}G^{jl}\dot{\eta}_{kl} + \frac{vE}{(1+v)(1-2v)} G^{ij}G^{kl}\dot{\eta}_{kl}$$

$$- (\sigma^{ik}G^{jl}\dot{\eta}_{kl} + \sigma^{jk}G^{il}\dot{\eta}_{kl}) \quad \text{if } \sigma_e < c,$$

$$\text{or } \sigma_e = c \text{ and } s^{ij}\dot{\eta}_{ij} \leqslant 0 \qquad (15)b$$

The field equations are now complete for analyzing large deformation problems. Note that the Kirchhoff stress q^{ij} appears in the equations of equilibrium whereas the constitutive equations involve σ^{ij}. In the present analysis, however, q^{ij} can be approximated by σ^{ij}. For small deformations, $G \cong g$, so that $q^{ij} = \frac{G}{g} \sigma^{ij} \cong \sigma^{ij}$. In the necking problem large deformations occur, but since the plastic strain, which is incompressible, dominates the elastic strain, the volume change caused by the total strain is very small. Then, since $\frac{G}{g} = \frac{dV}{dV} \cong 1$, it is still true that $q^{ij} \cong \sigma^{ij}$. Therefore, q^{ij} will be replaced by σ^{ij} in the equations of equilibrium for simplicity.

Finally, by the use of the constitutive equation (15) we can obtain another version of the variational statement that turns out to be convenient for numerical analysis. It can be easily verified that

$$\dot{\sigma}^{ij}\delta\eta_{ij} = \delta\dot{\sigma}^{ij}\eta_{ij}$$

both for plastic loading and unloading. Therefore, if I is defined by

$$I = \frac{1}{2}\int_V (\dot{\sigma}^{ij}\eta_{ij} + \sigma^{ij}[g_{st}(\dot{u}^s_i)(\dot{u}^t_j)])dV - \int_{S_T} \dot{T}^i\dot{u}_i\, dS \qquad (16)$$

where S_T is the part of the original surface on which traction rates are prescribed, then

$$\delta I = 0$$

is the same as the variational equation (6).

III. A Perfect Bar Under Uniaxial Tension

Before we go into the necking problem, let us study the uniform deformation of a perfect circularly cylindrical bar under uniaxial tension. The bar has an initial length 2L and an initial radius R_0 as shown in Fig. 3. The ends of the specimen are subjected to a prescribed uniform axial displacement U_L. The radial displacement at the ends is unrestrained so that the ends remain shear free during the elongation. The following is the solution for the uniform deformation of the perfect bar; this solution will be used for further comparison.

The physical axial displacement of the specimen is

$$u_z = a \cdot z$$

where $a = \dfrac{U_L}{L}$ is the engineering axial strain. The natural axial strain is $\bar{\eta} = \ln(1 + a)$. For a given engineering strain a, the uniaxial stress in the specimen can be calculated by the uniaxial stress-strain relation. In this paper, we will use the Ramberg-Osgood law [13] to relate the uniaxial true stress σ_{zz} and the natural strain $\bar{\eta}$ as follows:

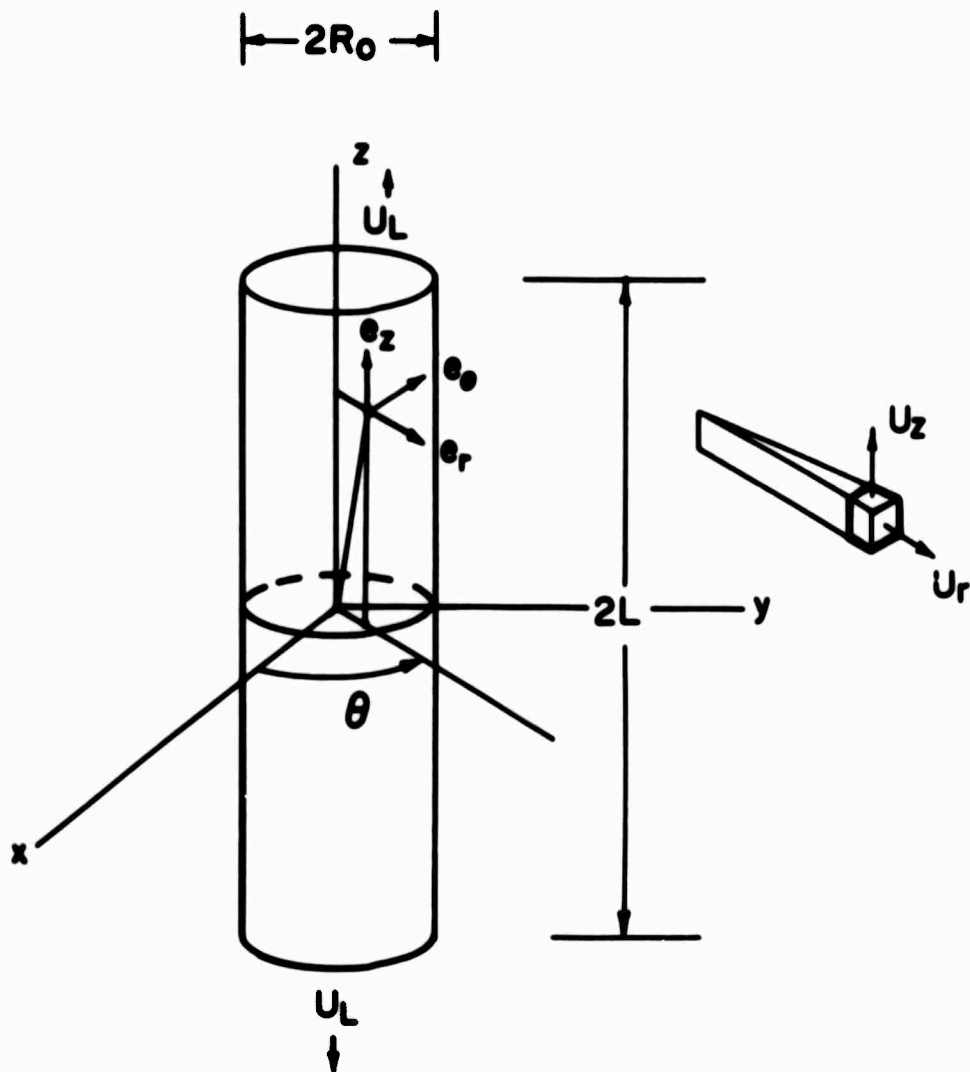$$\bar{\eta} = (\frac{\sigma_{zz}}{E}) + K(\frac{\sigma_{zz}}{E})^n \qquad (17)$$

FIG. 3 PERFECT BAR

where n is the strain-hardening exponent, and K is a material constant. As shown in [13], K is equal to $\frac{3}{7}(\frac{\sigma_s}{E})^{1-n}$, where σ_s is a secant yield strength at which the secant modulus $E_s = (\frac{\sigma_s}{\eta}) = .7E$. In the present analysis, it will be convenient to use the dimensionless stress quantity $(\frac{\sigma_{zz}}{\sigma_s})$. Rearranging equation (17) gives the following relation between $(\frac{\sigma_{zz}}{\sigma_s})$ and a given value of a:

$$(\frac{\sigma_s}{E})(\frac{\sigma_{zz}}{\sigma_s}) + \frac{3}{7}(\frac{\sigma_s}{E})(\frac{\sigma_{zz}}{\sigma_s})^n = \ln(1 + a) \qquad . \tag{17a}$$

The radial displacement is $u_r = br$, where the engineering radial strain b can be found by the use of the constitutive equation (10)a. Let η_{11} be the component of the Lagrangian strain tensor in the r direction and let σ^{33} be the only non-vanishing contravariant component of the stress tensor (i.e. consistant with the cylindrical coordinate system $\xi^1 = r$, $\xi^2 = \theta$, and $\xi^3 = z$); then $\eta_{11} = b + \frac{1}{2}b^2$ and $\sigma^{33}G_{33} = \sigma_3^3 = \sigma_e = \sigma_{zz}$. One of the constitutive relations of Eq. (10)a reduces to

$$\dot{\eta}_{11} = -\nu G_{11}(\frac{\sigma_s}{E})(\frac{\dot{\sigma}_{zz}}{\sigma_s}) - \frac{3}{14}nG_{11}(\frac{\sigma_s}{E})(\frac{\sigma_{zz}}{\sigma_s})^{n-1}(\frac{\dot{\sigma}_{zz}}{\sigma_s})$$

where the metric tensor $G_{11} = (1 + b)^2$. Integration of it gives

$$b = e^{-[\nu(\frac{\sigma_s}{E})(\frac{\sigma_{zz}}{\sigma_s})+\frac{3}{14}(\frac{\sigma_s}{E})(\frac{\sigma_{zz}}{\sigma_s})^n]} - 1 \qquad . \tag{18}$$

The radius of the specimen after deformation is $\overline{R} = R_0(1 + b)$. Next, the total load in dimensionless form is

$$\frac{T}{\pi R_0^2 \sigma_s} = (\frac{\sigma_{zz}}{\sigma_s})(1 + b)^2$$

$$= (\frac{\sigma_{zz}}{\sigma_s}) e^{-[2\nu(\frac{\sigma_s}{E})(\frac{\sigma_{zz}}{\sigma_s})+\frac{3}{7}(\frac{\sigma_s}{E})(\frac{\sigma_{zz}}{\sigma_s})^n]} \qquad . \tag{19}$$

Note that the values of b, $(\frac{\sigma_{zz}}{\sigma_s})$ and $(\frac{T}{\pi R_0^2 \sigma_s})$ depend on three material parameters only; namely, the strain-hardening exponent n, the ratio $(\frac{\sigma_s}{E})$ and Poisson's ratio ν.

For the particular values $n = 8$, $(\frac{\sigma_s}{E}) = 0.0072$ (consistant with the values $E = 25.8 \times 10^6$ psi. and $\sigma_s = .186 \times 10^6$ psi. for Cr-Ni steel), and $\nu = \frac{1}{3}$, curves relating a and $\frac{T}{\pi R_0^2 \sigma_s}$, and $\bar{R}$ and $\frac{T}{\pi R_0^2 \sigma_s}$ are plotted in Fig. 4 and Fig. 5. A very simple approximation for the maximum value of the total load (found by neglecting elastic strains) is

$$(\frac{T}{\pi R_0^2 \sigma_s})_{max} = [\frac{3}{7} ne(\frac{\sigma_s}{E})]^{-\frac{1}{n}}$$

and the corresponding values for the stress and engineering strains are

$$(\frac{\sigma_{zz}}{\sigma_s})_{T=Tmax} = [\frac{3}{7}n(\frac{\sigma_s}{E})]^{-\frac{1}{n}}$$

$$(a)_{T=Tmax} = e^{\frac{1}{n}} - 1$$

$$(b)_{T=Tmax} = e^{-\frac{1}{2n}} - 1 .$$

This approximation should hold fairly well for $n > 2$ and $n(\frac{\sigma_s}{E}) \ll 1$. For $n = 8$, for example, $(a)_{T=Tmax}$ is .133 and the corresponding natural axial strain is $(\bar{\eta})_{T=Tmax} = .125$.

IV. Formulation of the Necking Problem

The tension specimen considered for the present necking problem is an imperfect bar as shown in Fig. 6, of which the lateral surfaces deviate slightly from the straight surfaces of the perfect bar of Fig. 3. The initial length of this imperfect bar is again 2L, but its initial radius
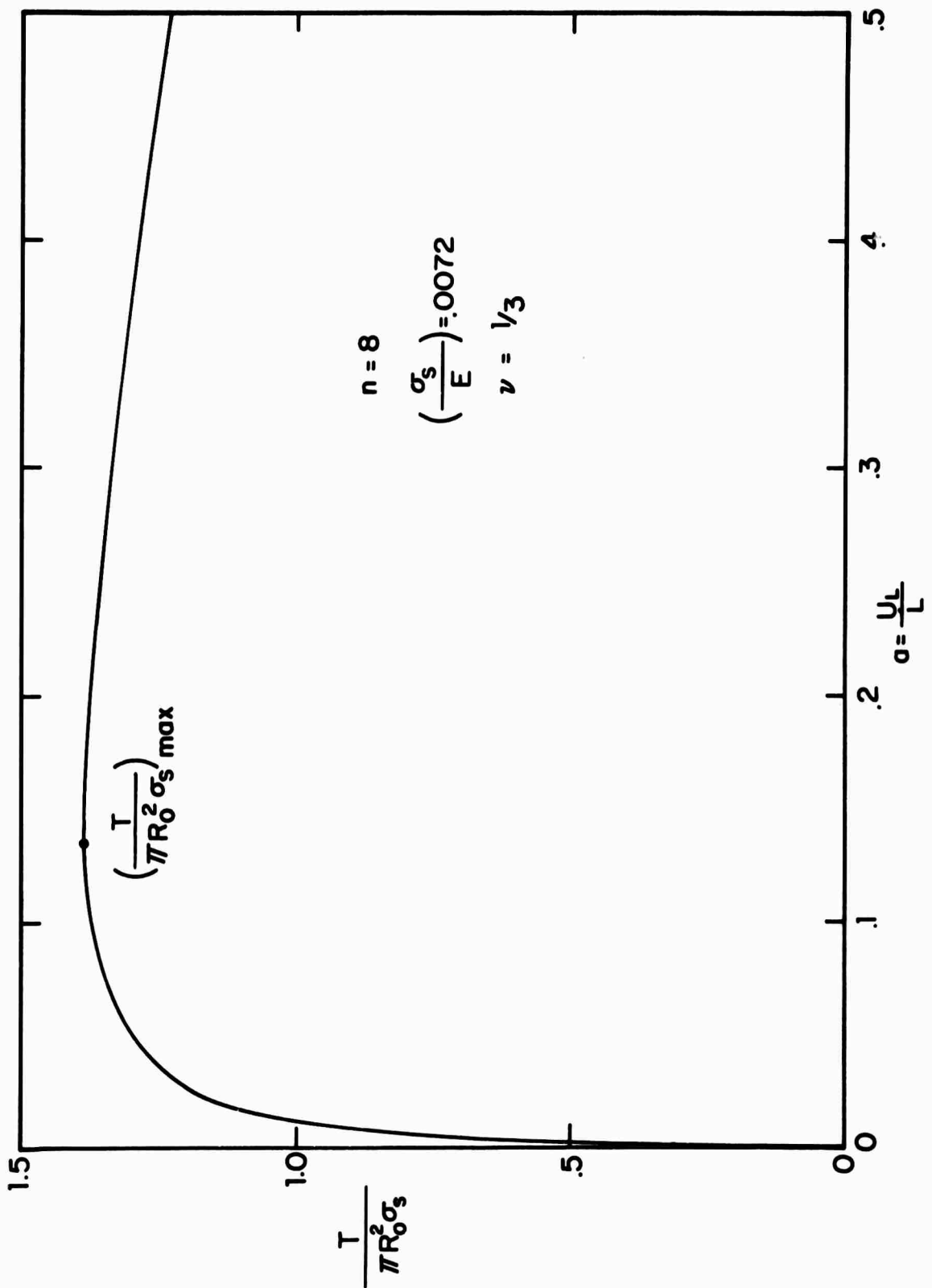
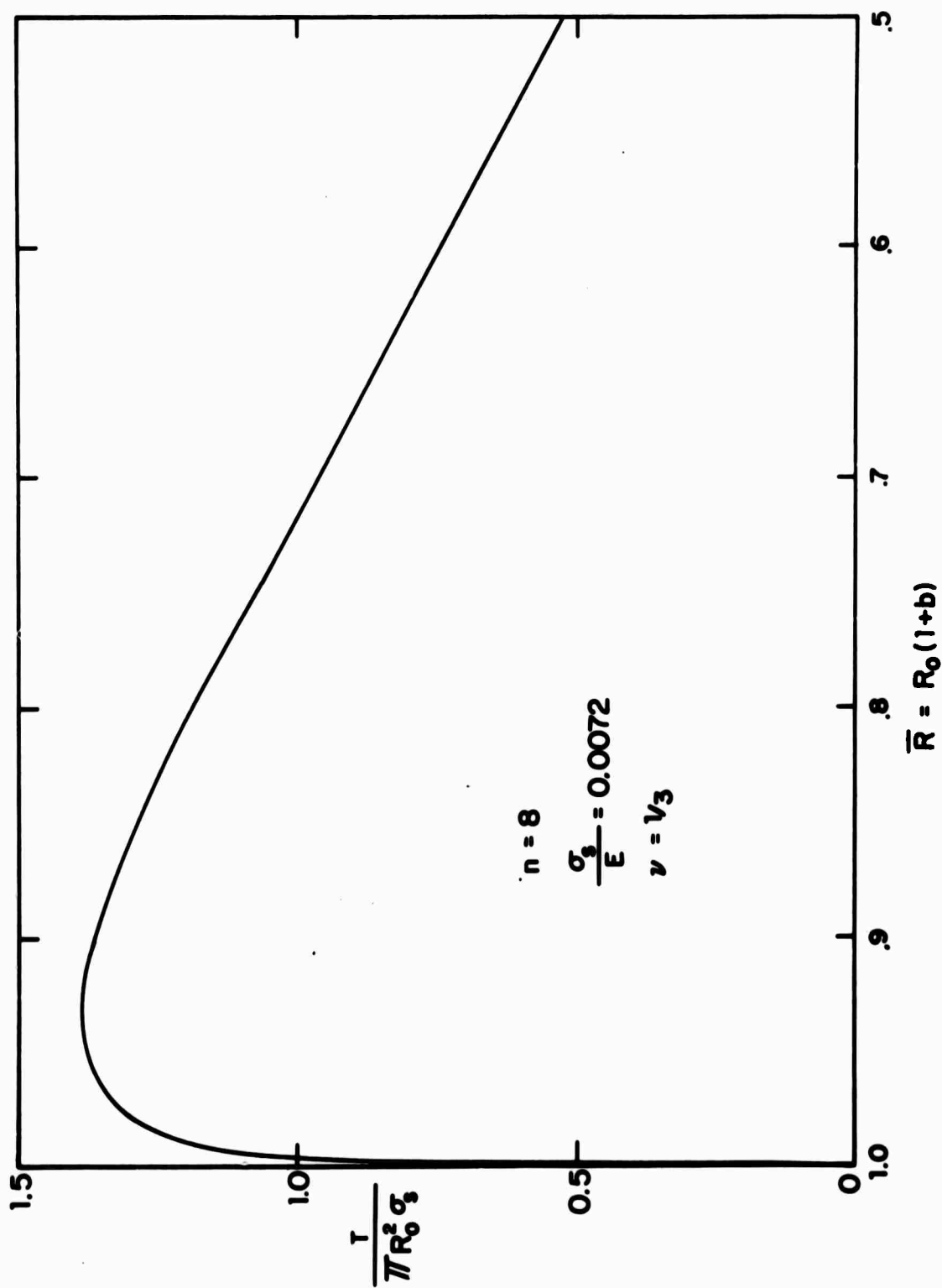FIG. 4 TOTAL LOAD VS. ENGINEERING AXIAL STRAIN FOR PERFECT BAR

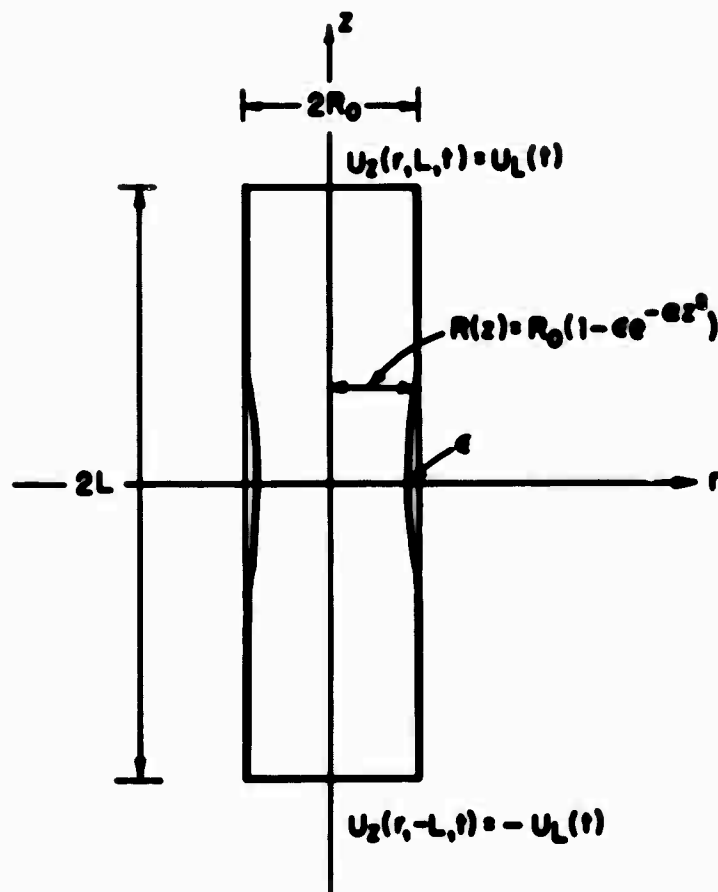FIG. 5 TOTAL LOAD VS. CURRENT RADIUS FOR PERFECT BAR (R_0=1)

$\overline{R} = R_0(1+b)$

$n = 8$

$\dfrac{\sigma_s}{E} = 0.0072$

$\nu = \nu_3$

$\dfrac{T}{\pi R_0^2 \, \sigma_s}$

FIG. 6 INITIALLY IMPERFECT BAR

is $R(z) = R_0(1 - \epsilon e^{-a z^2})$, where ϵ (assumed small) is the maximum deviation between the surfaces of the perfect and imperfect bar at $z = 0$, and a is a positive decay parameter.

The specimen is assumed to be axisymmetric about the z-axis and to be symmetric with respect to the middle plane $z = 0$. The only non-vanishing physical components of displacement are u_r and u_z, perpendicular and parallel to the z-axis, respectively. The non-vanishing physical components of stress are σ_{rr}, $\sigma_{\theta\theta}$, σ_{zz} and σ_{rz}. The stress and displacement components are functions of r and z and the time-like variable t; they are independent of θ by axial symmetry. The boundary conditions imposed at the ends are the same as those imposed on the perfect bar; namely, at the ends, $u_z(r, \pm L, t) = \pm U_L(t)$. Also, the radial displacement at the ends is unrestrained so that the ends remain shear free during the elongation.

Referred to the cylindrical coordinates (r, θ, z), the metric tensor g_{ij} has components

$$g_{ij} = \begin{bmatrix} g_{11} & g_{12} & g_{13} \\ g_{21} & g_{22} & g_{23} \\ g_{31} & g_{32} & g_{33} \end{bmatrix} = \begin{bmatrix} 1 & 0 & 0 \\ 0 & r^2 & 0 \\ 0 & 0 & 1 \end{bmatrix} .$$

The contravariant and covariant components of the displacement are

$$u^1 = u_1 = u_r$$

$$u^3 = u_3 = u_z$$

and the stress tensor has contravariant components

$$\sigma^{ij} = \begin{bmatrix} \sigma^{11} & 0 & \sigma^{13} \\ 0 & \sigma^{22} & 0 \\ \sigma^{31} & 0 & \sigma^{33} \end{bmatrix} .$$

The rates of the Lagrangian strain tensor components are

$$\dot{\eta}_{11} = (1 + \frac{\partial u_r}{\partial r}) \frac{\partial \dot{u}_r}{\partial r} + \frac{\partial u_z}{\partial r} \frac{\partial \dot{u}_z}{\partial r}$$

$$\dot{\eta}_{22} = (r + u_r)\dot{u}_r$$

$$\dot{\eta}_{33} = (1 + \frac{\partial u_z}{\partial z}) \frac{\partial \dot{u}_z}{\partial z} + \frac{\partial u_r}{\partial z} \frac{\partial \dot{u}_r}{\partial z} \tag{20}$$

$$\dot{\eta}_{13} = \dot{\eta}_{31} = \frac{1}{2}(1 + \frac{\partial u_z}{\partial z})\frac{\partial \dot{u}_z}{\partial r} + \frac{1}{2}(1 + \frac{\partial u_r}{\partial r})\frac{\partial \dot{u}_r}{\partial z} + \frac{1}{2}(\frac{\partial u_r}{\partial z}\frac{\partial \dot{u}_r}{\partial r} + \frac{\partial u_z}{\partial r}\frac{\partial \dot{u}_z}{\partial z}).$$

The covariant components of the metric tensor of the deformed body are

$$G_{11} = (1 + \frac{\partial u_r}{\partial r})^2 + (\frac{\partial u_z}{\partial r})^2$$

$$G_{22} = (r + u_r)^2$$

$$G_{33} = (1 + \frac{\partial u_z}{\partial z})^2 + (\frac{\partial u_r}{\partial z})^2 \tag{21}$$

$$G_{13} = G_{31} = (\frac{\partial u_r}{\partial z} + \frac{\partial u_z}{\partial r}) + (\frac{\partial u_r}{\partial r}\frac{\partial u_r}{\partial z} + \frac{\partial u_z}{\partial r}\frac{\partial u_z}{\partial z})$$

with the inverses

$$G^{11} = \frac{G_{33}}{(G_{11}G_{33} - G_{13})^2}$$

$$G^{22} = \frac{1}{G_{22}}$$

$$G^{33} = \frac{G_{11}}{(G_{11}G_{33} - G_{13})^2} \tag{22}$$

$$G^{13} = G^{31} = \frac{-G_{13}}{(G_{11}G_{33} - G_{13})^2}$$

The non-vanishing contravariant components of the stress deviator, s^{11}, s^{22}, s^{33} and s^{13}, are given by

$$s^{ij} = \sigma^{ij} - \frac{1}{3}G^{ij}(\sigma^{11}G_{11} + \sigma^{22}G_{22} + \sigma^{33}G_{33} + 2\sigma^{13}G_{13}) \qquad (23)$$

The effective stress is

$$\sigma_e = \{\frac{1}{2}[(\sigma^{11})^2 G_{11}^2 + (\sigma^{22})^2 G_{22}^2 + (\sigma^{33})^2 G_{33}^2 + 2(\sigma^{13})^2 G_{13}^2$$

$$+ 2(\sigma^{13})^2 G_{11}G_{33} + 2\sigma^{11}\sigma^{33}G_{13}^2 + 4\sigma^{11}\sigma^{13}G_{11}G_{13}$$

$$+ 4\sigma^{13}\sigma^{33}G_{13}G_{33}]\}^{\frac{1}{2}} \qquad . \qquad (24)$$

For the present problem, let us continue to use the Ramberg-Osgood law (17) as the uniaxial true stress-natural strain relation. The tangent modulus by definition is

$$\frac{1}{E_t} = \frac{\dot{\eta}}{\dot{\sigma}_e} = \frac{1}{E} + \frac{1}{E}\frac{3}{7}n(\frac{\sigma_e}{\sigma_s})^{n-1} \qquad . \qquad (25)$$

In the following we will use the convenient dimensionless stress quantity $(\frac{\sigma^{ij}}{\sigma_s})$ and also the dimensionless quantities $(\frac{\sigma_e}{\sigma_s})$ and $(\frac{\eta_e}{\eta_s})$. Substitution of (25) into (15) gives

$$(\frac{\sigma^{ij}}{\sigma_s}) = \frac{1}{(1+v)}(\frac{E}{\sigma_s})[G^{ik}G^{jl}\dot{\eta}_{kl} - P(\frac{\sigma_e}{\sigma_s})\cdot(\frac{\sigma^{ij}}{\sigma_s})(\frac{\sigma^{kl}}{\sigma_s})\dot{\eta}_{kl}]$$

$$+ \frac{v}{(1+v)(1-2v)}(\frac{E}{\sigma_s})G^{ij}G^{kl}\dot{\eta}_{kl} - [(\frac{\sigma^{ik}}{\sigma_s})G^{jl}\dot{\eta}_{kl} + (\frac{\sigma^{jk}}{\sigma_s})G^{il}\dot{\eta}_{kl}]$$

$$(26)$$

where

$$P(\frac{\sigma_e}{\sigma_s}) = \begin{cases} \dfrac{27n(\frac{\sigma_e}{\sigma_s})^{n-3}}{28(1+v) + 18n(\frac{\sigma_e}{\sigma_s})^{n-1}} & \text{if } \sigma_e = c \text{ and } s^{ij}\dot{\eta}_{ij} > 0 \qquad (27)a \\[4mm] 0 & \text{if } \sigma_e < c, \text{ or } \sigma_e = c \text{ and} \\ & \qquad s^{ij}\dot{\eta}_{ij} < 0 \qquad (27)b \end{cases}$$

The constitutive relations in matrix form are

$$
\begin{array}{c}
\dfrac{\epsilon^{11}}{\sigma_s} \\[2mm]
\dfrac{\epsilon^{22}}{\sigma_s} \\[2mm]
\dfrac{\epsilon^{33}}{\sigma_s} \\[2mm]
\dfrac{\epsilon^{13}}{\sigma_s}
\end{array}
\qquad
\begin{array}{cccc c}
C_{11} & C_{12} & C_{13} & C_{14} & h_{11} \\[2mm]
C_{21} & C_{22} & C_{23} & C_{24} & h_{22} \\[2mm]
C_{31} & C_{32} & C_{33} & C_{34} & h_{33} \\[2mm]
C_{41} & C_{42} & C_{43} & C_{44} & 2h_{13}
\end{array}
\qquad (28)
$$

where the coefficients C_{ij} are

$$
C_{11} = \frac{1}{1+\nu}\left(\frac{E}{\sigma_s}\right)\left[\frac{1-\nu}{1-2\nu}(G^{11})^2 - \left(\frac{s^{11}}{\sigma_s}\right)^2 P\left(\frac{\sigma_e}{\sigma_s}\right)\right] - 2\left(\frac{\epsilon^{11}}{\sigma_s}\right)G^{11}
$$

$$
C_{22} = \frac{1}{1+\nu}\left(\frac{E}{\sigma_s}\right)\left[\frac{1-\nu}{1-2\nu}(G^{22})^2 - \left(\frac{s^{22}}{\sigma_s}\right)^2 P\left(\frac{\sigma_e}{\sigma_s}\right)\right] - 2\left(\frac{\epsilon^{22}}{\sigma_s}\right)G^{22}
$$

$$
C_{33} = \frac{1}{1+\nu}\left(\frac{E}{\sigma_s}\right)\left[\frac{1-\nu}{1-2\nu}(G^{33})^2 - \left(\frac{s^{33}}{\sigma_s}\right)^2 P\left(\frac{\sigma_e}{\sigma_s}\right)\right] - 2\left(\frac{\epsilon^{33}}{\sigma_s}\right)G^{33}
$$

$$
C_{44} = \frac{1}{2(1+\nu)}\left(\frac{E}{\sigma_s}\right)\left[G^{11}G^{33} + \frac{1}{1-2\nu}(G^{13})^2 - 2\left(\frac{s^{13}}{\sigma_s}\right)^2 P\left(\frac{\sigma_e}{\sigma_s}\right)\right]
$$

$$
- \frac{1}{2}\left[\left(\frac{\epsilon^{11}}{\sigma_s}\right)G^{33} + 2\left(\frac{\epsilon^{13}}{\sigma_s}\right)G^{13} + \left(\frac{\epsilon^{33}}{\sigma_s}\right)G^{11}\right]
$$

$$
C_{12} = C_{21} = \frac{1}{1+\nu}\left(\frac{E}{\sigma_s}\right)\left[\frac{\nu}{1-2\nu}G^{11}G^{22} - \left(\frac{s^{11}}{\sigma_s}\right)\left(\frac{s^{22}}{\sigma_s}\right)P\left(\frac{\sigma_e}{\sigma_s}\right)\right]
$$

$$
C_{13} = C_{31} = \frac{1}{1+\nu}\left(\frac{E}{\sigma_s}\right)\left[(G^{13})^2 + \frac{\nu}{1-2\nu}G^{11}G^{33} - \left(\frac{s^{11}}{\sigma_s}\right)\left(\frac{s^{33}}{\sigma_s}\right)P\left(\frac{\sigma_e}{\sigma_s}\right)\right]
$$

$$
- 2\left(\frac{\epsilon^{13}}{\sigma_s}\right)G^{13}
$$

$$C_{14} = C_{41} = \frac{1}{1+\nu}(\frac{E}{\sigma_s})[\frac{1-\nu}{1-2\nu}G^{11}G^{13} - (\frac{s^{11}}{\sigma_s})(\frac{s^{13}}{\sigma_s})P(\frac{\sigma_e}{\sigma_s})]$$

$$- [(\frac{s^{11}}{\sigma_s})G^{13} + (\frac{s^{13}}{\sigma_s})G^{11}]$$

$$C_{23} = C_{32} = \frac{1}{1+\nu}(\frac{E}{\sigma_s})[\frac{\nu}{1-2\nu}G^{22}G^{33} - (\frac{s^{22}}{\sigma_s})(\frac{s^{33}}{\sigma_s})P(\frac{\sigma_e}{\sigma_s})]$$

$$C_{24} = C_{42} = \frac{1}{1+\nu}(\frac{E}{\sigma_s})[\frac{\nu}{1-2\nu}G^{22}G^{13} - (\frac{s^{22}}{\sigma_s})(\frac{s^{13}}{\sigma_s})P(\frac{\sigma_e}{\sigma_s})]$$

$$C_{34} = C_{43} = \frac{1}{1+\nu}(\frac{E}{\sigma_s})[\frac{1-\nu}{1-2\nu}G^{13}G^{33} - (\frac{s^{13}}{\sigma_s})(\frac{s^{33}}{\sigma_s})P(\frac{\sigma_e}{\sigma_s})]$$

$$- [(\frac{s^{13}}{\sigma_s})G^{33} + (\frac{s^{33}}{\sigma_s})G^{13}] \quad . \tag{29}$$

With the use of the constitutive equation (28), the equation (16) of the variational principle becomes

$$\frac{1}{\sigma_s} = 2\pi \int_0^L \int_0^{R(z)} \{C_{11}h_{11}^2 + C_{22}h_{22}^2 + C_{33}h_{33}^2 + 4C_{44}h_{13}^2 + 2C_{12}h_{11}h_{22}$$

$$+ 2C_{13}h_{11}h_{33} + 4C_{14}h_{11}h_{13} + 2C_{23}h_{22}h_{33} + 4C_{24}h_{22}h_{13}$$

$$+ 4C_{34}h_{33}h_{13} + (\frac{s^{11}}{\sigma_s})[(\frac{\partial \dot u_r}{\partial r})^2 + (\frac{\partial \dot u_z}{\partial r})^2] + (\frac{s^{22}}{\sigma_s})(\dot u_r)^2$$

$$+ (\frac{s^{33}}{\sigma_s})[(\frac{\partial \dot u_r}{\partial z})^2 + (\frac{\partial \dot u_z}{\partial z})^2] + 2(\frac{s^{13}}{\sigma_s})[\frac{\partial \dot u_r}{\partial r}\frac{\partial \dot u_r}{\partial z} + \frac{\partial \dot u_z}{\partial r}\frac{\partial \dot u_z}{\partial z}]\} r\,dr\,dz \quad .$$

$$\tag{30}$$

The surface integral of (16) vanishes, since the prescribed tractions vanish on all boundaries. Equation (30), with the use of the strain-displacement relation (20) can be written in the form

$$\frac{1}{\sigma_s} = 2\pi \int_0^L \int_0^{R(z)} [\text{Quadratic terms in } \dot{u}_r, \dot{u}_z, \text{ and their derivatives}] r\,dr\,dz \quad . \tag{31}$$

The variational principle $\delta I = 0$, with the I of (31), will enable one to solve for $\dot{u}_r$ and $\dot{u}_z$.

Finally, the geometric boundary conditions that must be imposed on the displacements are

$$\dot{u}_z(r, L, t) = \dot{U}_L(t) \tag{32}$$

at the end, and

$$\dot{u}_z(r, 0, t) = 0 \tag{33}$$

at the middle, by symmetry.

V. Method of Solution and Numerical Analysis

The governing equations of the present problem were approximately solved by the Kantorovich approach [5] based on the variational principle $\delta I = 0$, where I is given by Equation (31). In this method the displacements were assumed in the form

$$u_r = rf(z, t) + r^3 h(z, t) \tag{34}$$

$$u_z = g(z, t) + r^2 k(z, t) \tag{35}$$

where f, h, g, and k are functions of the space variable z as well as the time t. The axisymmetric conditions require that equation (34) contain only odd powers of r and that equation (35) contain only even powers of r.

To analyze the necking process, we must calculate the stress σ^{ij} and the displacement u_i as functions of r, z and t. The details of this calculation will be shown later; the following paragraph outlines briefly the computation steps involved in the procedure.

Assuming knowledge of the histories of σ^{ij} and u_i at time t, calculate the displacement rate $(\dot{u}_i)_t$ by the variational equation for a prescribed axial displacement rate $\dot{U}_L$ at the end. Then calculate $(\dot{\eta}_{ij})_t$ and $(\dot{\sigma}^{ij})_t$ by the strain-displacement relations and the constitutive equations, respectively. Next, extrapolate to find $(\sigma^{ij})_{t+\Delta t}$ and $(u_i)_{t+\Delta t}$, and then use this knowledge to calculate $(\dot{u}_i)_{t+\Delta t}$. Repeat the same procedure for successive small time intervals and thus obtain the stress and displacement histories for a finite time span.

By this procedure, the displacement functions f, g, h, and k of Equations (34) and (35) are assumed to be known at time t, and it is their rates $\dot{f}$, $\dot{g}$, $\dot{h}$, and $\dot{k}$ that are the unknowns to be found. Substitution of the assumed displacements (34) and (35) into the equations (20) for the rates of the Lagrangian strain tensor components gives

$$\dot{\eta}_{11} = (1 + f + 3r^2h)(\dot{f} + 3r^2\dot{h}) + 4r^2k\dot{k}$$

$$\dot{\eta}_{22} = (1 + f + r^2h)(\dot{f} + r^2\dot{h})$$

$$\dot{\eta}_{33} = r^2(f_z + r^2h_z)(\dot{f}_z + r^2\dot{h}_z) + (1 + g_z + r^2k_z)(\dot{g}_z + r^2\dot{k}_z)$$

$$\dot{\eta}_{13} = \dot{\eta}_{31} = \frac{1}{2}r(f_z + r^2h_z)(\dot{f} + 3r^2\dot{h}) + \frac{1}{2}r(1 + f + 3r^2h)(\dot{f}_z + r^2\dot{h}_z)$$

$$+ rk(\dot{g}_z + r^2\dot{k}_z) + r(1 + g_z + r^2k_z)\dot{k} \quad . \tag{36}$$

With the use of these relations, the expression (31) for the integral I of the variational principle becomes

$$\frac{1}{\sigma_s} = \int_0^L [D_{11}\ddot{f}^2 + D_{12}\ddot{f}\ddot{f}_z + D_{13}\ddot{f}\ddot{h} + D_{14}\ddot{f}\ddot{h}_z + D_{15}\ddot{f}\ddot{g}_z + D_{16}\ddot{f}\ddot{k} + D_{17}\ddot{f}\ddot{k}_z$$

$$+ D_{22}\ddot{f}_z^2 + D_{23}\dot{f}_z\dot{h} + D_{24}\dot{f}_z\dot{h}_z + D_{25}\dot{f}_z\dot{g}_z + D_{26}\dot{f}_z\dot{k} + D_{27}\dot{f}_z\dot{k}_z$$

$$+ D_{33}\dot{h}^2 + D_{34}\ddot{h}\ddot{h}_z + D_{35}\ddot{h}\ddot{g}_z + D_{36}\ddot{h}\ddot{k} + D_{37}\ddot{h}\ddot{k}_z$$

$$+ D_{44}\dot{h}_z^2 + D_{45}\dot{h}_z\dot{g}_z + D_{46}\dot{h}_z\dot{k} + D_{47}\dot{h}_z\dot{k}_z$$

$$+ D_{55}\dot{g}_z^2 + D_{56}\dot{g}_z\dot{k} + D_{57}\dot{g}_z\dot{k}_z$$

$$+ D_{66}\dot{k}^2 + D_{67}\ddot{k}\ddot{k}_z$$

$$+ D_{77}\dot{k}_z^2]dz \qquad (37)$$

where the coefficients $D_{\alpha\beta}$ are definite integrals with respect to r. For example

$$D_{11} = 2\pi \int_0^{R(z)} \{C_{11}(1 + f + 3r^2h)^2 + C_{22}(1 + f + r^2h)^2$$

$$+ 2C_{12}(1 + f + 3r^2h)(1 + f + r^2h) + 2C_{14}r(1 + f + 3r^2h)(f_z + r^2h_z)$$

$$+ 2C_{24}r(1 + f + r^2h)(f_z + r^2h_z) + C_{44}r^2(f_z + r^2h_z)^2$$

$$+ \sigma^{11} + \sigma^{22}r^2\}rdr$$

$$D_{12} = 2\pi \int_0^{R(z)} \{2(C_{13} + C_{44})r^2(1 + f + 3r^2h)(f_z + r^2h_z)$$

$$+ 2C_{23}r^2(1 + f + r^2h)(f_z + r^2h_z) + 2C_{14}r(1 + f + 3r^2h)^2$$

$$+ 2C_{24}r(1 + f + r^2h)(1 + f + 3r^2h) + 2C_{34}r^3(f_z + r^2h_z)^2$$

$$+ 2r\sigma^{13}\}rdr \quad .$$

The rest of these 28 coefficients are calculated in a similar fashion, but the results are not shown here. All the $D_{\alpha\beta}$ are, of course, functions of z.

The condition $\delta I = 0$ can then be imposed in order to solve for $\dot{f}$, $\dot{g}$, $\dot{h}$, and $\dot{k}$, as functions of z. Let the integral domain of (37); namely, the plane bounded by $z = 0$, L and $r = 0$, R(z), be divided into m x n meshes, with m + 1 mesh points in the r direction and n + 1 mesh points in the z direction (see Fig. 7). Numerical calculation at time t starts by the computation of G_{ij}, G^{ij}, S^{ij}, σ_e and C_{ij} by means of Equations (21), (22), (23), (24), and (29) at each mesh point. In computing C_{ij}, we have to know whether a mesh point is governed by the plastic loading conditions or by the plastic unloading conditions in order to calculate $P(\frac{\sigma_e}{\sigma_s})$ by (27)a or (27)b, respectively. However, before the solutions for $\dot{u}_i$ are found, these plastic loading or unloading conditions cannot be checked, and hence the position of the boundary between the plastic loading region and the plastic unloading region is not known. In the present analysis, this boundary is determined by an iterative process which will be described later. For now we just assume a trial position of the boundary in the specimen and calculate $P(\frac{\sigma_e}{\sigma_s})$ either by (27)a or (27)b. After C_{ij} is evaluated at each mesh point, we integrate numerically along the r direction by Simpson's rule to get the $D_{\alpha\beta}$ of (37). Then let the discrete values of f, g, h, k and $D_{\alpha\beta}$ at z_i (i^{th} mesh point along the z-axis) be f_i, g_i, h_i, k_i and $(D_{\alpha\beta})_i$. By the use of the trapezoidal rule, Equation (37) can be written approximately in the summation form

$$I = \sum_{1}^{n} I_i [\text{Quadratic terms in } \dot{f}_i, \dot{f}_{i+1}, \dot{g}_i, \dot{g}_{i+1}, \dot{h}_i, \dot{h}_{i+1}, \dot{k}_i, \dot{k}_{i+1},$$

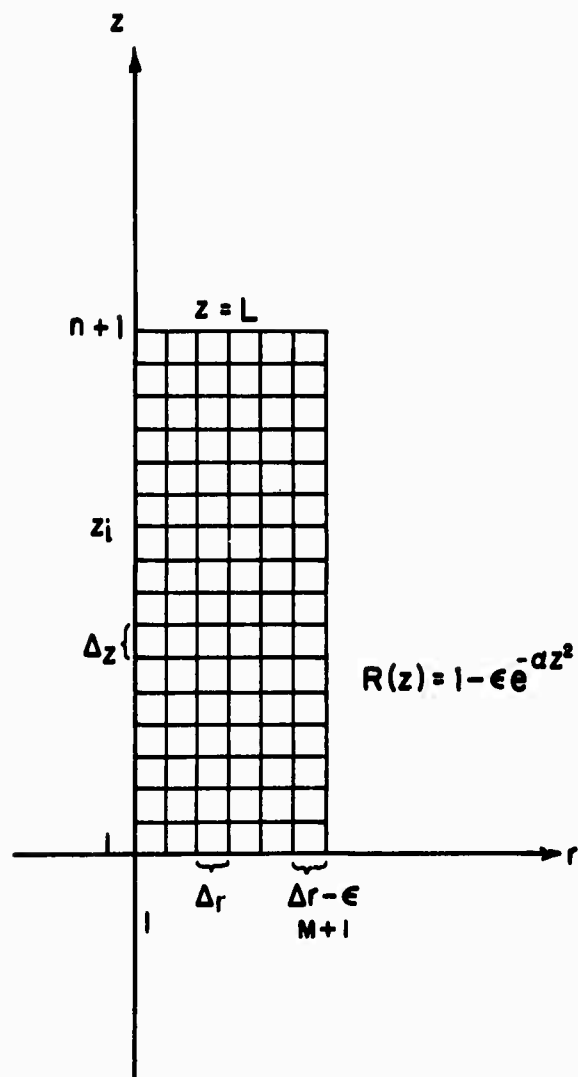$$(D_{\alpha\beta})_i \text{ and } (D_{\alpha\beta})_{i+1}] \quad . \tag{38}$$

FIG. 7 GRID FOR NUMERICAL
COMPUTATION

The variational principle $\delta I = 0$, with the I of (38), implies that

$$\frac{\partial I}{\partial \dot{f}_i} = 0$$

$$\frac{\partial I}{\partial \dot{g}_i} = 0$$

$$\frac{\partial I}{\partial \dot{h}_i} = 0$$

$$\frac{\partial I}{\partial \dot{k}_i} = 0 \tag{39}$$

for $i = 2$ to n. The natural boundary conditions of the variational principle are

$$\frac{\partial I}{\partial \dot{f}_1} = 0$$

$$\frac{\partial I}{\partial \dot{h}_1} = 0 \tag{40}$$

at the middle $z = 0$, and

$$\frac{\partial I}{\partial \dot{f}_{n+1}} = 0$$

$$\frac{\partial I}{\partial \dot{h}_{n+1}} = 0 \tag{41}$$

at the end $z = L$. In addition, the geometric boundary conditions (32) and (33) become

$$\dot{g}_1 = 0$$

$$\dot{k}_1 = 0$$

$$\dot{g}_{n+1} = \dot{U}_L$$

$$\dot{k}_{n+1} = 0 \qquad . \tag{42}$$

Equations (39), (40), (41) and (42) constitute a system of $4(n + 1)$ linear equations which contain $4(n + 1)$ unknowns $\dot{f}_i$, $\dot{g}_i$, $\dot{h}_i$ and $\dot{k}_i$ (for $i = 1$ to $n + 1$). These equations were solved by Potter's method (see Ref. 14) with the aid of an IBM 360/65 computer. After $\dot{f}_i$, $\dot{g}_i$, $\dot{h}_i$ and $\dot{k}_i$ are found, the displacement rates $\dot{u}_r$ and $\dot{u}_z$ can be calculated by means of (34) and (35).

The calculated displacement rates $\dot{u}_r$ and $\dot{u}_z$ are not necessarily the correct solution, because they were obtained on the basis of an assumed position for the boundary between the plastic loading and plastic unloading region. So after we calculate $\dot{\eta}_{ij}$ from $\dot{u}_i$, we must check the plastic loading conditions—namely, $\sigma_e = c$ (c is the maximum value of σ_e which has occurred in the stress history) and $\dot{\eta}_{ij}s^{ij} \neq 0$—at each mesh point in the assumed plastic loading region. If these conditions are not satisfied, we redefine the mesh point assumed to be plastically loading to plastically unloading. Similarly, we check the plastic unloading condi- tions—namely, $\sigma_e < c$, or $\sigma_e = c$ and $\dot{\eta}_{ij}s^{ij} \leq 0$—for each mesh point in the assumed plastic unloading region and make the required adjustment if necessary. Thus we obtain a new position of the boundary. Then we calculate $\dot{u}_i$ on the basis of the new boundary and do the checking again. If this checking is successful, the last displacement rate $\dot{u}_i$ found is taken as the right solution. From these values for $\dot{u}_i$, the strain rate $\dot{\eta}_{ij}$ and the stress rate $(\dfrac{\dot{\sigma}^{ij}}{\sigma_s})$ are calculated by (36) and (28), successively.

The stress and the displacement at the time $t + \Delta t$ are estimated by a simple parabolic extrapolation of the form

$$u_{t+\Delta t} = u_t + [\tfrac{3}{2}\dot{u}_t - \tfrac{1}{2}\dot{u}_{t-\Delta t}]\Delta t$$

assuming a knowledge of the various rates at the time $t - \Delta t$ (initially at $t = 0$, it suffices to use $u_{\Delta t} = \dot{u}_0 \Delta t$ if Δt is sufficiently small). For convenience, the time-like variable t was identified as the prescribed end displacement $U_L(t)$, so that $\dot{U}_L = 1$ and $\Delta T = \Delta U_L$.

Finally, after the tensor components of stress were found, the physical components of stress were calculated. At the neck, where shear strain does not occur, the dimensionless physical components of stress are simply:

$$\frac{\sigma_{rr}}{\sigma_s} = \frac{\sigma^{11}}{\sigma_s} \quad \bar{G}_{11} \quad \bar{G}_{11}$$

$$\frac{\sigma_{\theta\theta}}{\sigma_s} = \frac{\sigma^{22}}{\sigma_s} \quad G_{22} \quad G_{22}$$

$$\frac{\sigma_{zz}}{\sigma_s} = \frac{\sigma^{33}}{\sigma_s} \cdot G_{33} \setminus \bar{G}_{33}$$

$$\frac{\sigma_{rz}}{\sigma_s} = \frac{\sigma^{13}}{\sigma_s} \cdot \bar{G}_{11} \quad G_{33} = 0$$

The dimensionless total load $\dfrac{T}{\pi R_0^2 \sigma_s}$ was calculated at the neck by integrating $\left(\dfrac{\sigma_{zz}}{\sigma_s}\right)$ over the current area $\bar{A}$ of the neck; namely,

$$\frac{T}{\pi R_0^2 \sigma_s} = \frac{1}{\pi R_0^2} \int \left(\frac{\sigma_{zz}}{\sigma_s}\right) d\bar{A} \quad . \tag{43}$$

Since $d\bar{A} = 2\pi(r + u_r)d(r + u_r) = 2\pi(1 + f + r^2 h)(1 + f + 3r^2 h)rdr$, equation (43) becomes

$$\frac{T}{\pi R_0^2 \sigma_s} = \frac{2}{R_0^2} \int_0^{R_0 - \epsilon} \frac{\sigma_{zz}}{\sigma_s}(1 + f + r^2 h) \cdot (1 + f + 3r^2 h)rdr \tag{44}$$

with f and h being evaluated at $z = 0$. The value of the total load was then obtained by the numerical integration of (44).

VI. Results and Discussions

The results presented are based on the following conditions. The initial half-length of the specimen is $L = 2$, and the initial radius is $R(z) = 1 - \epsilon e^{-z^2}$, with the imperfection arbitrarily chosen as $\epsilon = 0.005$ (the results are not sensitive to the magnitude of ϵ). The strain-hardening exponent is $n = 8$, the ratio $(\frac{\sigma_s}{E})$ is 0.0072 ($E = 25.7 \times 10^6$ psi. and $\sigma_s = .186 \times 10^6$ psi.), and Poisson's ratio is $\nu = \frac{1}{3}$. The results include the total load, the displacements and the stress and strain distributions calculated at every stage of deformation. Each stage of deformation was specified by a different value of the engineering axial strain $\frac{U_L}{L}$. In the present paper $\frac{U_L}{L}$ was varied with increment .0025, from 0 to .50, at which point the calculation was terminated for reasons which will be given later. The spatial mesh sizes used in the numerical analysis were $\Delta_r = .05$ and $\Delta_z = .025$.

6.1. The total load

Fig. 8 shows a plot of the dimensionless total load $\frac{T}{\pi R_0^2 \sigma_s}$ (as calculated by (44)) against the engineering strain $\frac{U_L}{L}$. The total load reaches its maximum at $\frac{U_L}{L} = 0.145$. It is interesting to notice that the plastic unloading (which starts at the ends of the bar) does not begin until $\frac{U_L}{L}$ reaches 0.180, which is slightly after the total load has started decreasing.

For comparison, the plot of $\frac{T}{\pi R_0^2 \sigma_s}$ versus $\frac{U_L}{L}$ as shown in Fig. 4 for the perfect bar was reproduced in Fig. 8. It is seen that the maximum value of the total load of the imperfect bar agrees quite well with that predicted for the perfect bar. The discrepancy between the two total loads begins shortly after the total loads start decreasing.
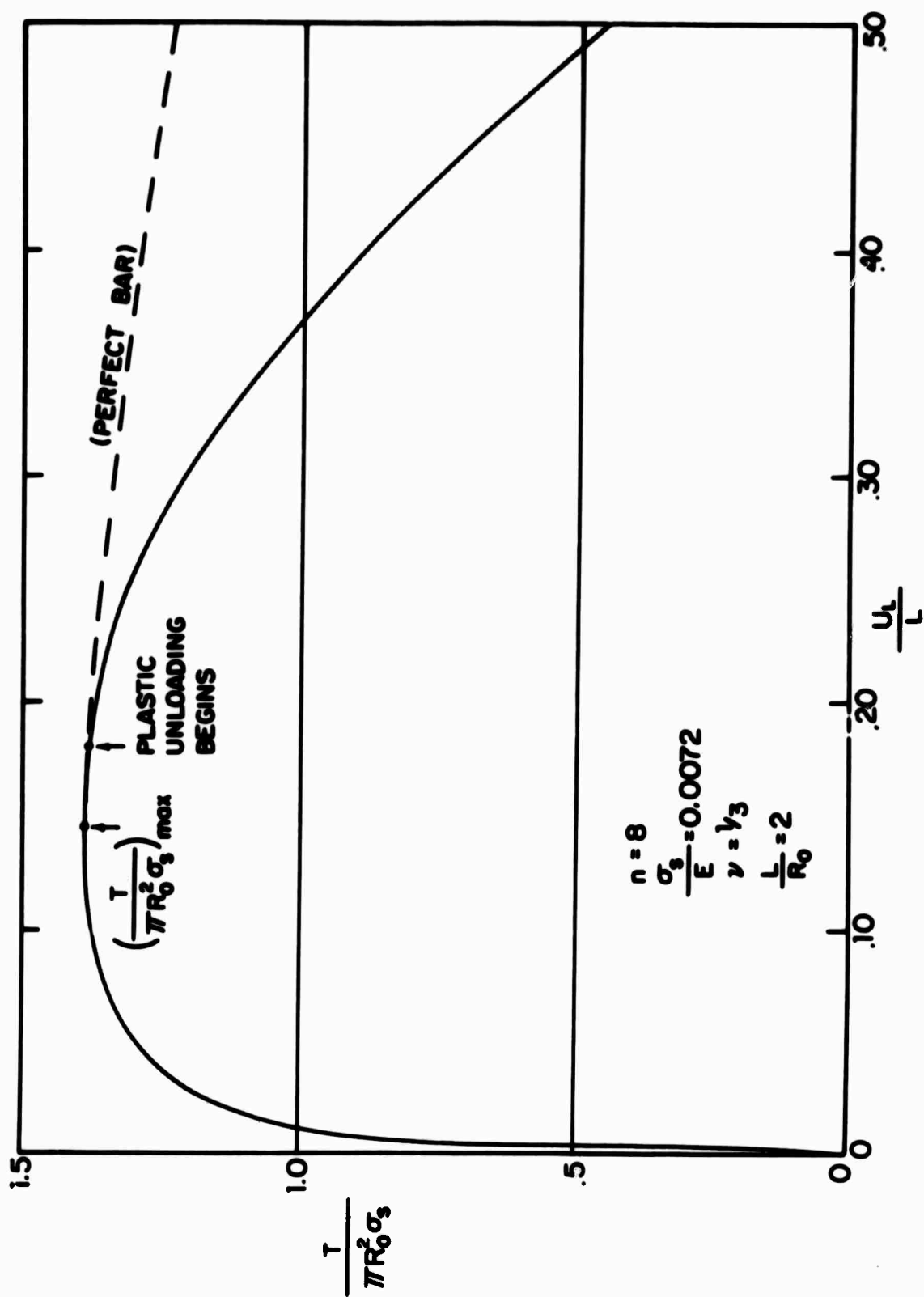
FIG. 8 TOTAL LOAD VS. ENGINEERING AXIAL STRAIN

The relation between $\dfrac{T}{\pi R_0^2 \sigma_s}$ and the radius at the neck $\overline{R}$ is shown in Fig. 9. The results for the perfect bar were also reproduced from Fig. 5 for comparison.

6.2. The displacements and the deformations

Fig. 10 shows the radial displacement u_r on the lateral surface, $r = R(z)$, at different stages of deformation. During the earlier stages of deformation, the inward radial displacement increases quite uniformly throughout the length. But for later stages, the inward radial displacement increases only locally at the middle. At the end of the specimen the radius expands slightly when the total load decreases (see the enlargement in Fig. 10).

The axial displacement u_z is shown in Fig. 11 for different stages of deformation. In this figure the solid lines indicate the axial displacement on the lateral surface, $r = R(z)$, and the dashed lines show the axial displacement along the center line, $r = 0$. The slopes of these curves become much steeper at the middle for large values of $\dfrac{U_L}{L}$. This implies that the axial strain, which is approximately equal to the slope of these curves, becomes concentrated locally at the middle when the deformation is large.

The localization of the displacements at the middle of the specimen as shown in Fig. 10 and Fig. 11 can easily be explained qualitatively as follows. The radius at the middle is initially smaller than the radius at the ends due to the initial imperfection. As the elongation proceeds, the stress and strain at the middle cross-section are larger than at the end cross-sections; therefore, the discrepancy between the radii increases. When the rate of decrease of cross-sectional area exceeds the rate of
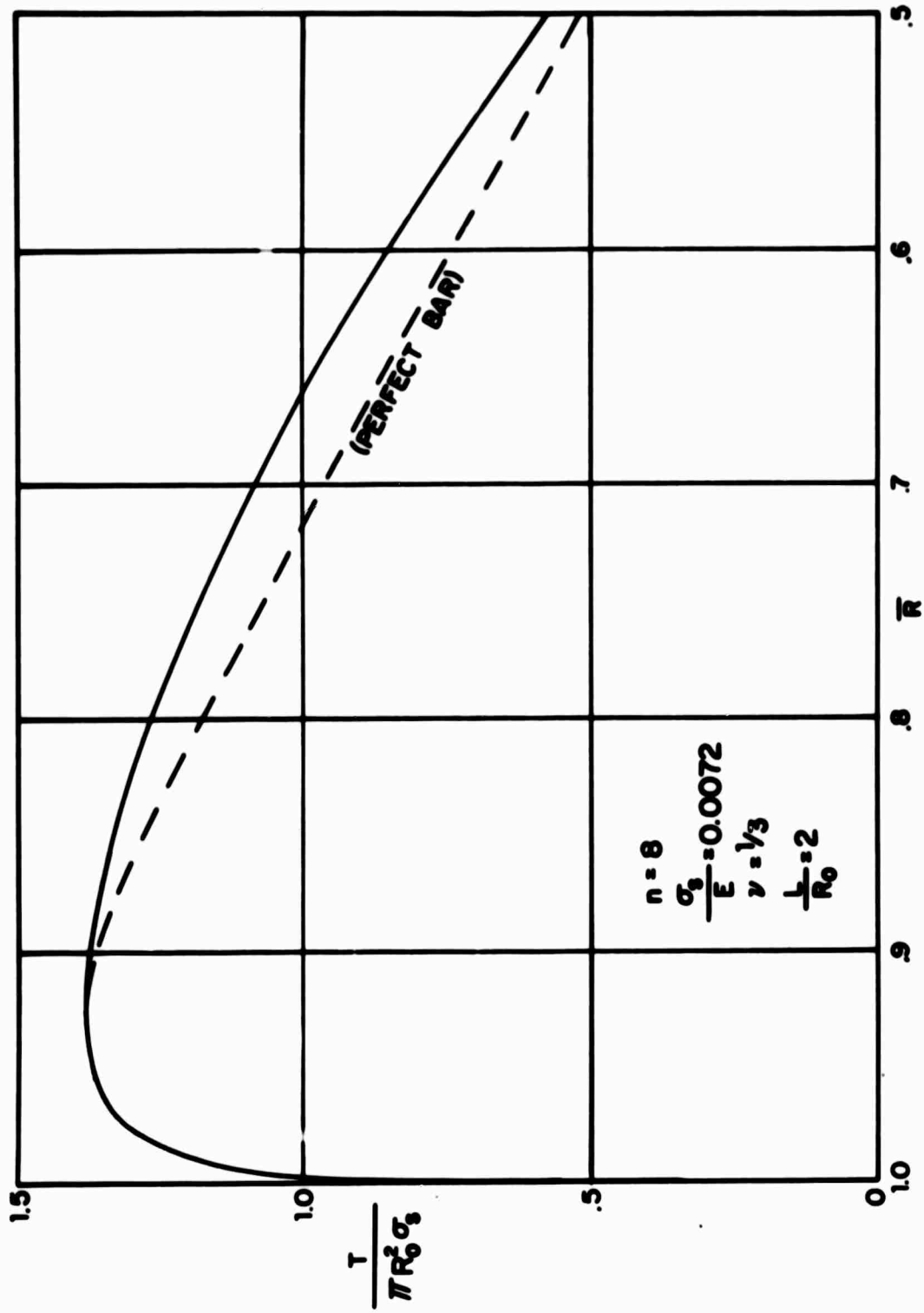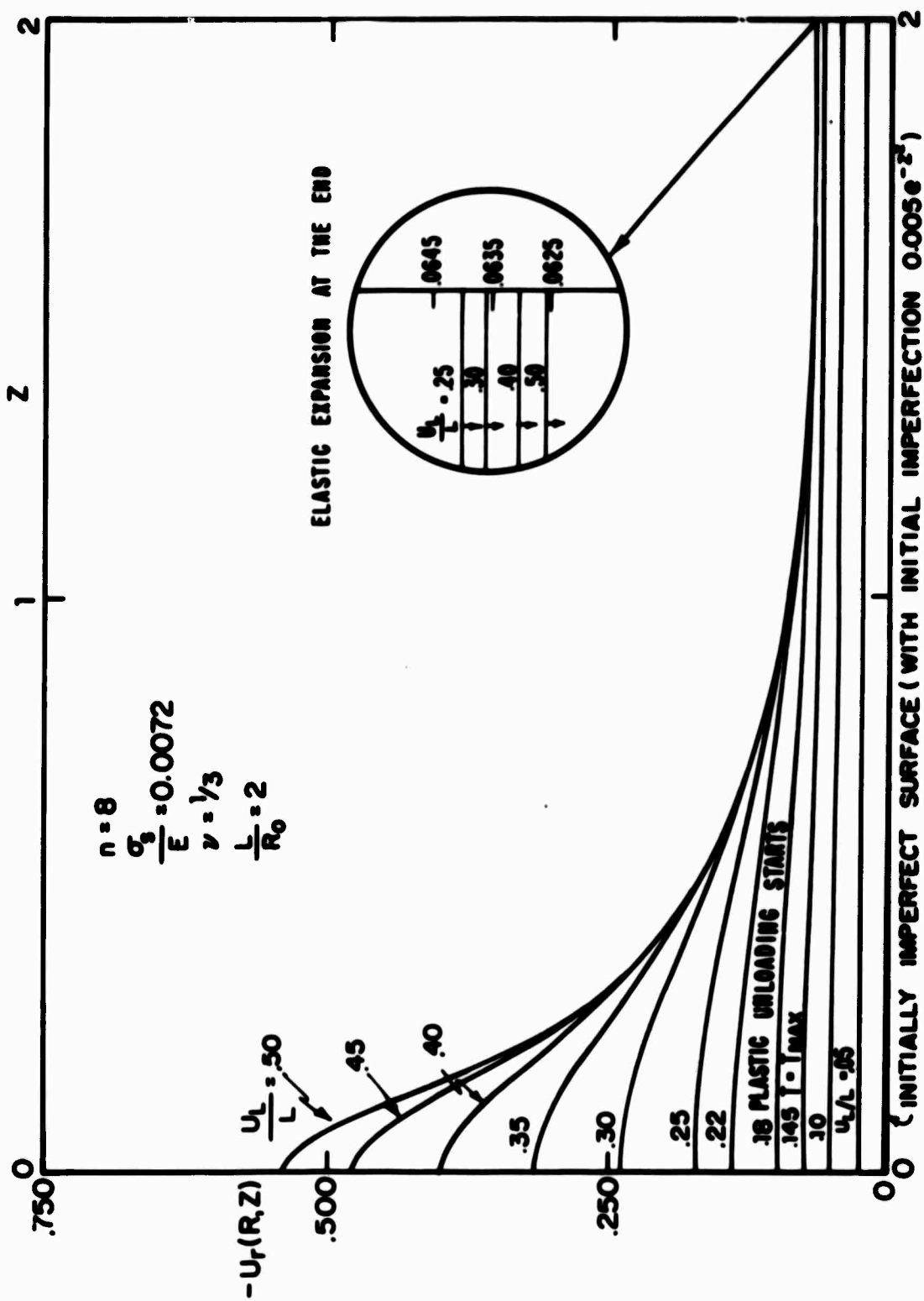
FIG. 9 TOTAL LOAD VS. NECK RADIUS
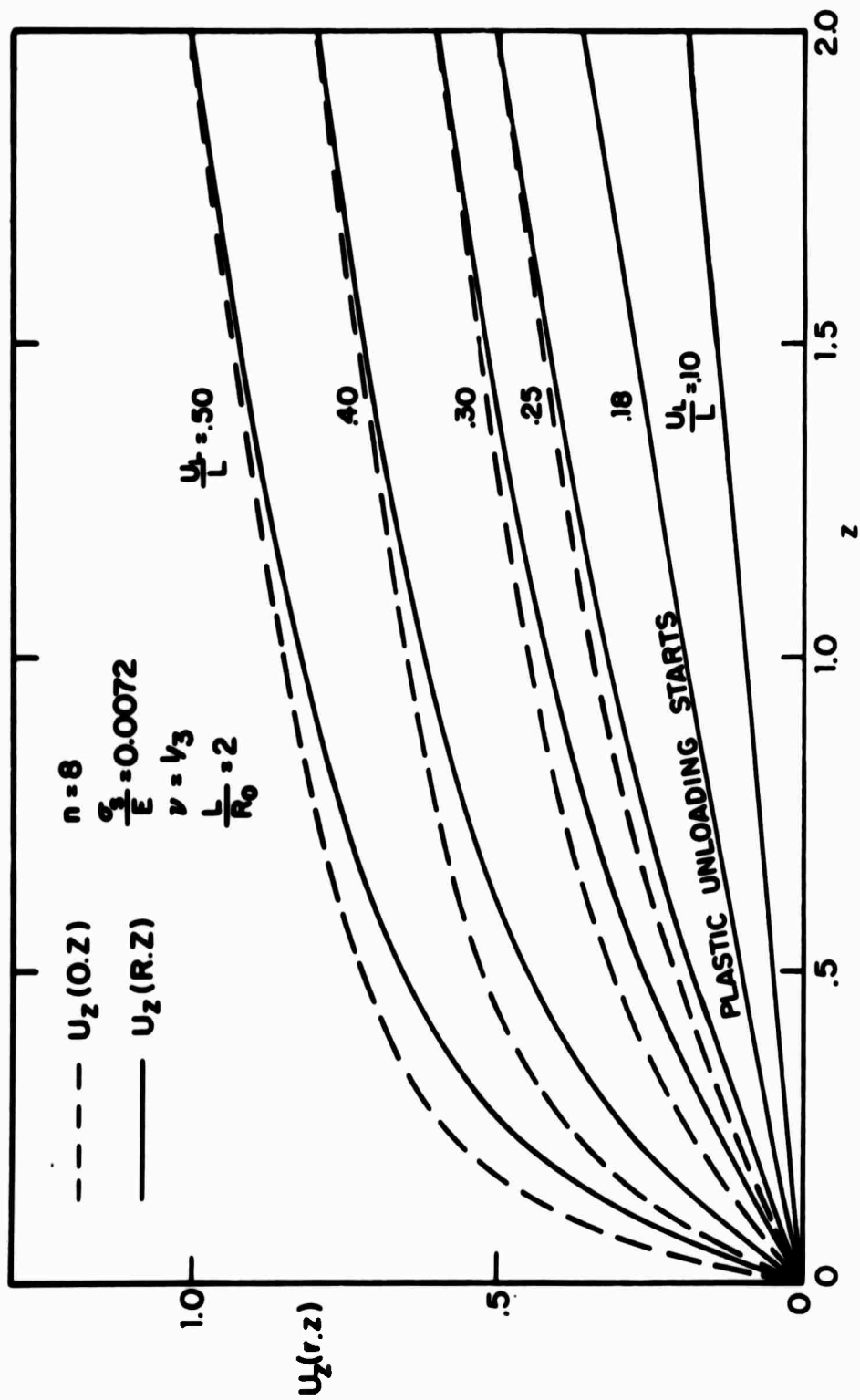
FIG. 10 RADIAL DISPLACEMENT ON LATERAL SURFACE
(INITIALLY IMPERFECT SURFACE (WITH INITIAL IMPERFECTION $0.005e^{-z^2}$))

FIG. II AXIAL DISPLACEMENT ON LATERAL SURFACE AND AT CENTER LINE

increase of the average axial stresses at the middle, the total load begins to decrease. Shortly after this, the effective stress decreases at the ends, and hence plastic unloading begins. Once the plastic un- loading occurs, the area contraction at the ends stops (in fact, the radii at the ends expand slightly as a result of the decrease of the axial stress); therefore, the discrepancy between the radii of the middle and the ends accelerates. As the elongation increases further, the stress at the neck becomes larger, but the cross-section contracts at an even faster rate, so that the total load decreases further. This results in larger plastic unloading regions at the ends and aggravates the discrepancy in the radii; thus, the displacements become localized at the middle.

The location of the boundary between the plastic unloading region and the plastic loading region is shown in Fig. 12 at different stages of deformation. To the left of this boundary is the plastic loading region and to the right of this boundary is the plastic unloading region. This boun- dary moves toward the middle as the total elongation increases.

From the knowledge of the displacements, the shapes of the necked- down specimen at different stages of deformation were calculated and are shown in Fig. 13. At $\frac{U_L}{L} = .50$, the localized necking results in a 53% reduction of the radius at the middle, while the reduction of the radius at the end is only about 6.3%. The detailed deformation in the specimen can be seen from Figs. 14 (a), (b) and (c). These figures show the de- formations of a square grid of the original body (see Fig. 7) at $\frac{U_L}{L} = 0.30$, 0.40 and 0.50.

The shapes of the necked profiles of the tension specimen shown ob- viously resemble the shapes observed in tests. However, no precise comparison has been made.
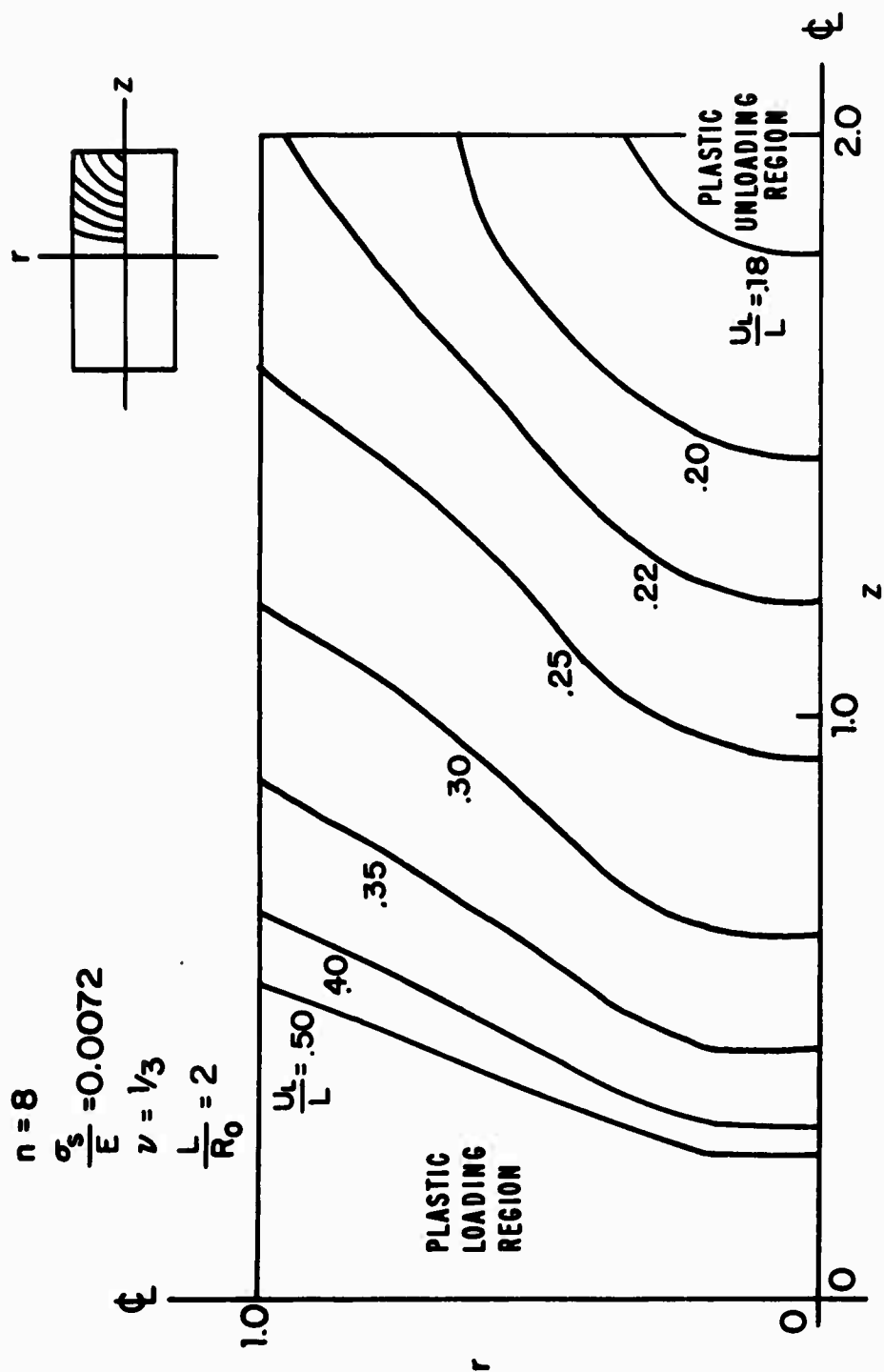
FIG. 12 BOUNDARY BETWEEN PLASTIC LOADING AND PLASTIC UNLOADING REGION
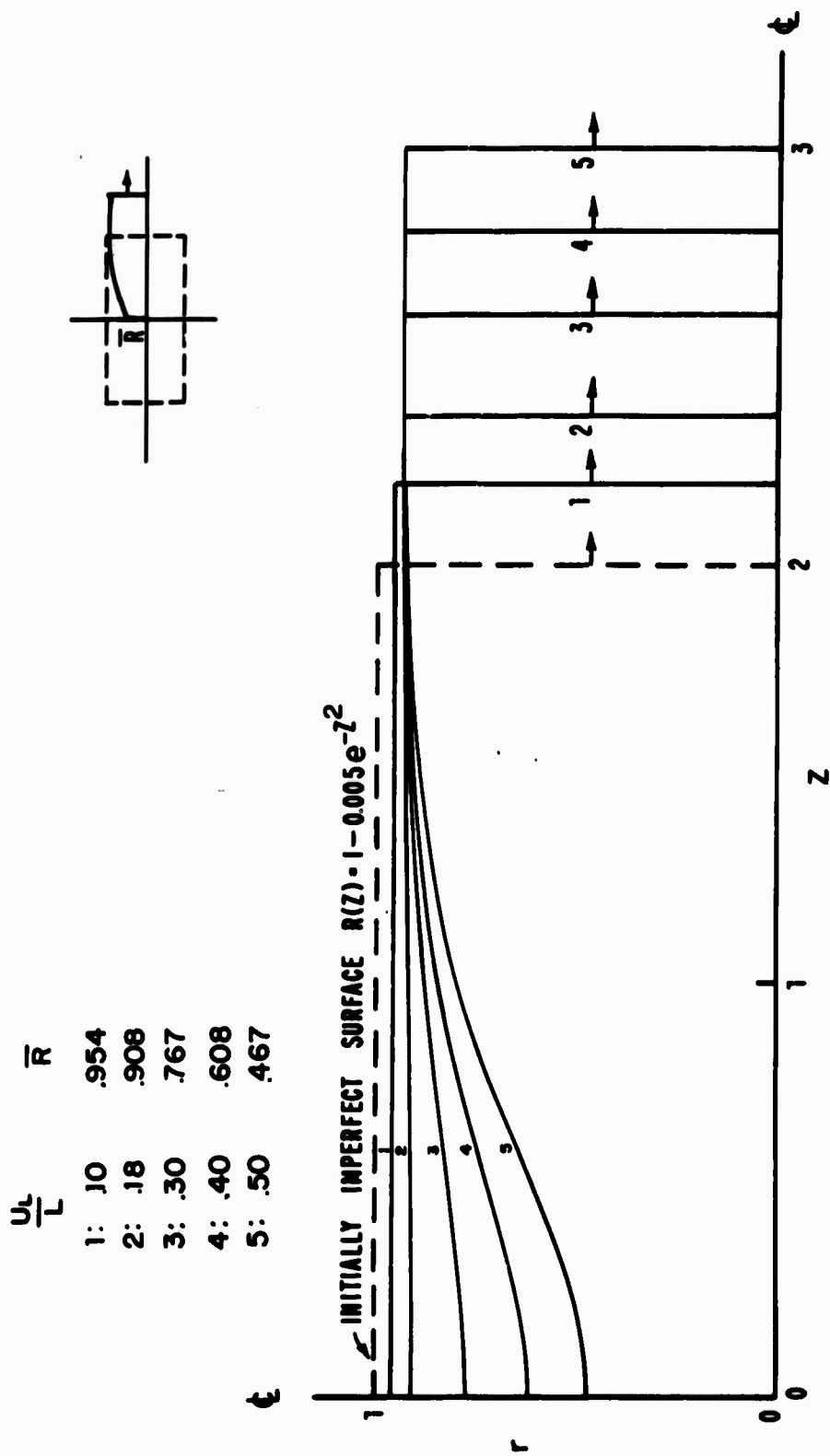
FIG. 13 NECKED SHAPES OF A TENSION SPECIMEN ($n=8$, $\frac{\sigma_3}{E}=0.0072$; $\nu=\frac{1}{3}$ AND $\frac{L}{R_0}=2$)
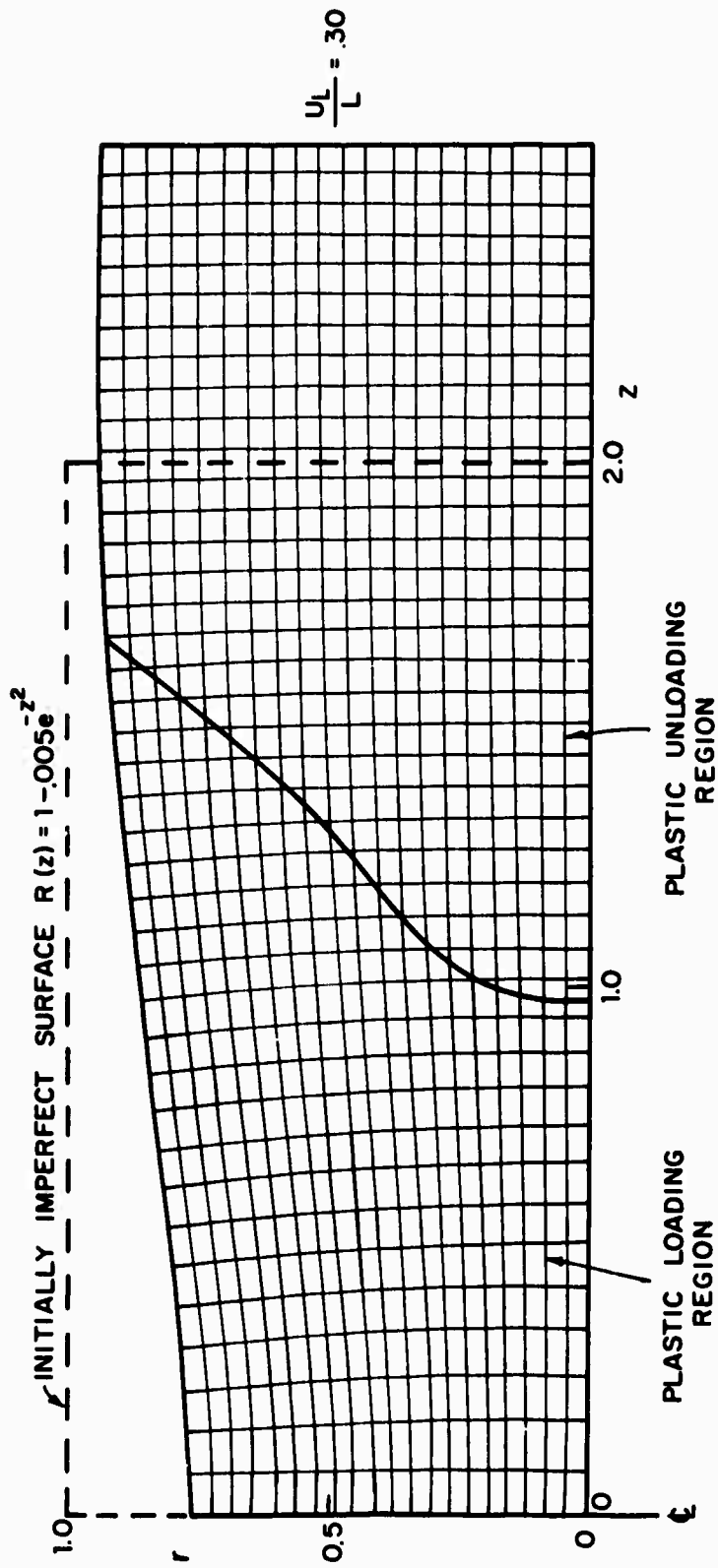
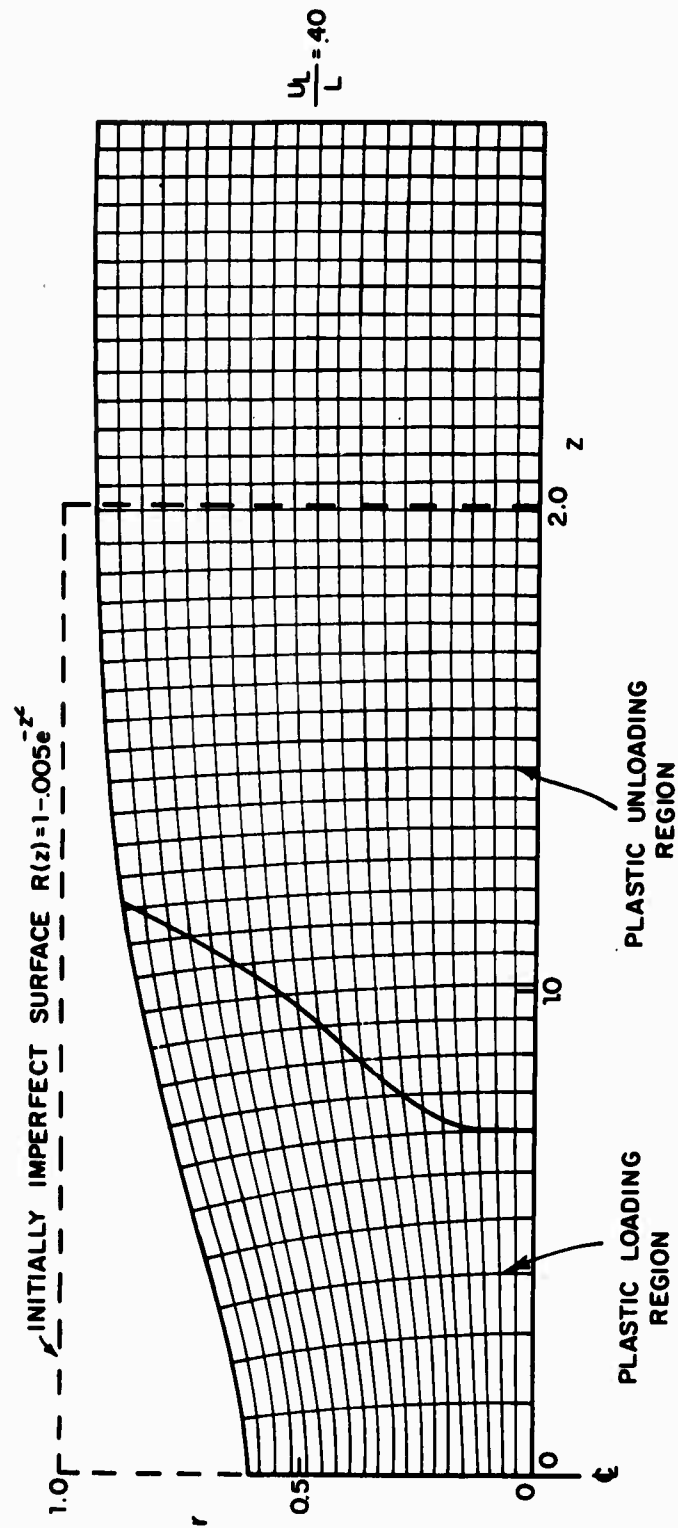FIG. 14A DEFORMATION OF AN INITIALLY SQUARE GRID AT $\frac{U_L}{L} = .30$

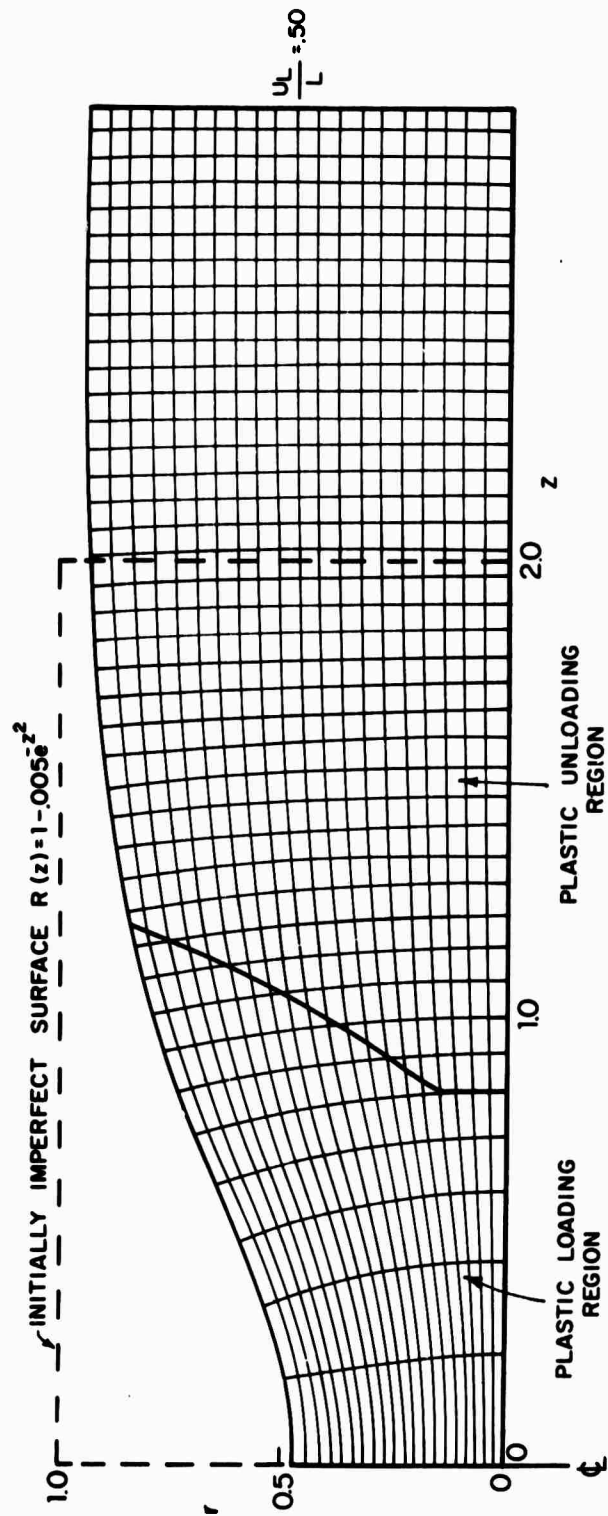FIG. 14B DEFORMATION OF AN INITIALLY SQUARE GRID AT $\frac{U_L}{L} = .40$

FIG. 14C DEFORMATION OF AN INITIALLY SQUARE GRID AT $\frac{U_L}{L} = .50$

6. 3. The strain and stress distributions

The stress and strain distributions have been calculated in the whole specimen during its loading history. Only some of these distributions at the neck will be shown.

Figs. 15, 16 and 17 show the Lagrangian strain tensor components across the neck section at $\frac{U_L}{L}$ = .25, .30, and .35. The maximum axial strain $(\eta_{33})_{max}$ is seen to occur at the center. It is interesting to recall that the Bridgman [1] and Davidenkov and Spiridonova [2] analyses were based on the assumption that the axial strain at the neck was uniform.

In the present analysis after the Lagrangian strain components are found, the value of $\sqrt{\frac{G}{g}}$, which was assumed to be close to 1 in order to use the approximation $\sigma^{ij} \cong q^{ij}$, was calculated. The maximum error of this assumption was found to be less than 1.5% for $\frac{U_L}{L}$ under .50.

The distributions of the physical components of stress, σ_{rr}, $\sigma_{\theta\theta}$, and σ_{zz}, at the neck are shown in Figs. 18a, 19a, and 20a for $\frac{U_L}{L}$ = .25, .30 and .35, and the distribution of the effective stress at these stages of deformation are shown in Fig. 18b, 19b, and 20b. The analysis showed that for $\frac{U_L}{L}$ less than .27, $(\sigma_{zz})_{max}$ occurs at the center as shown in Fig. 18a, and for $\frac{U_L}{L}$ over .27, $(\sigma_{zz})_{max}$ moves between the center and the peripheral surface as shown in Figs. 19a and 20a. The stress distributions shown may be inaccurate at comparatively large deformations, since then σ_{rr} does not vanish on the peripheral surface at the neck. (The requirement σ_{rr} = 0 on the peripheral surface at the neck is a natural boundary condition of the variational principle; to impose this condition is beyond the control of the present calculation process. The error in σ_{rr} on the surface can be used as a criterion for checking the accuracy; this accuracy can be improved by including more
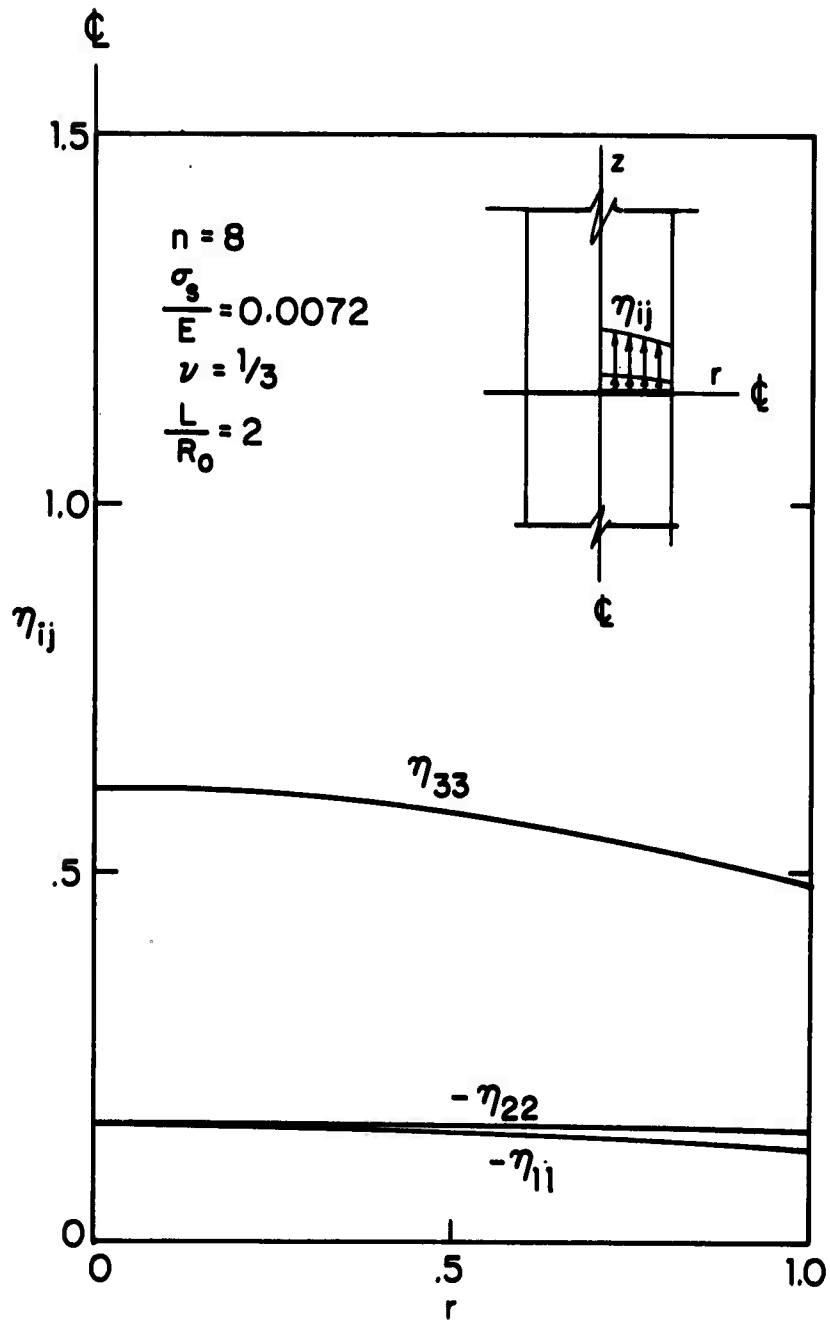
FIG. 15 LAGRANGIAN STRAIN COMPONENTS
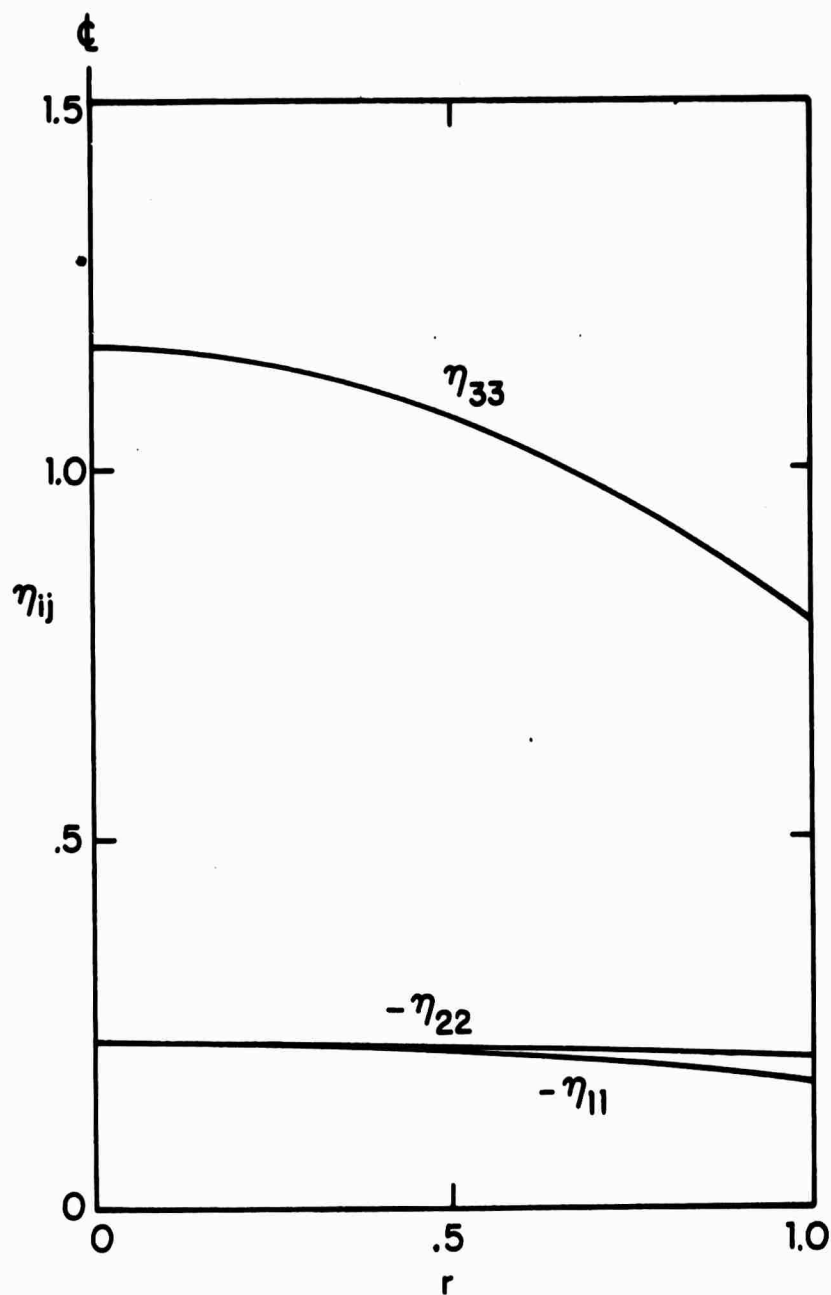AT THE NECK FOR $\frac{U_L}{L}$ = .25

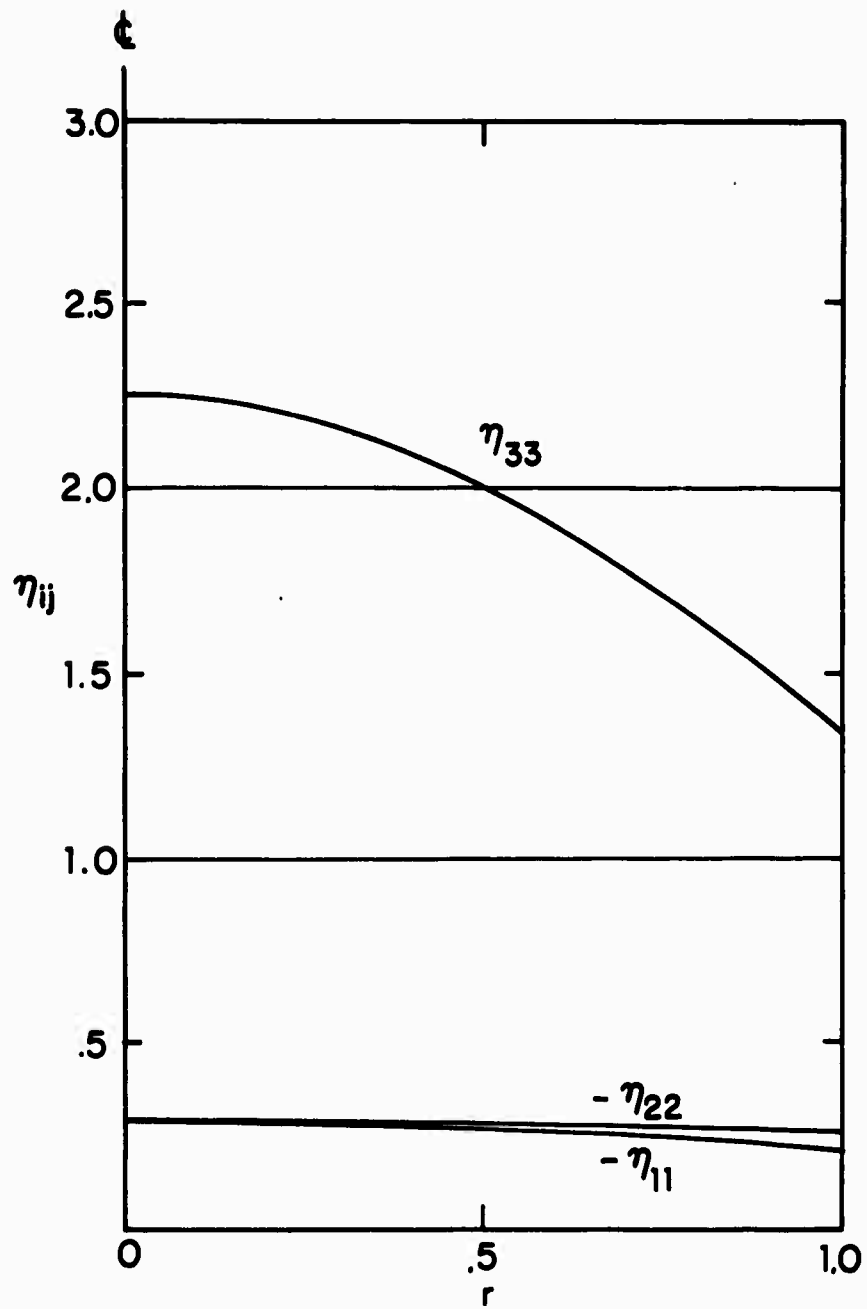FIG. 16 LAGRANGIAN STRAIN COMPONENTS AT THE NECK FOR $\frac{U_L}{L} = .30$

FIG. 17 LAGRANGIAN STRAIN COMPONENTS
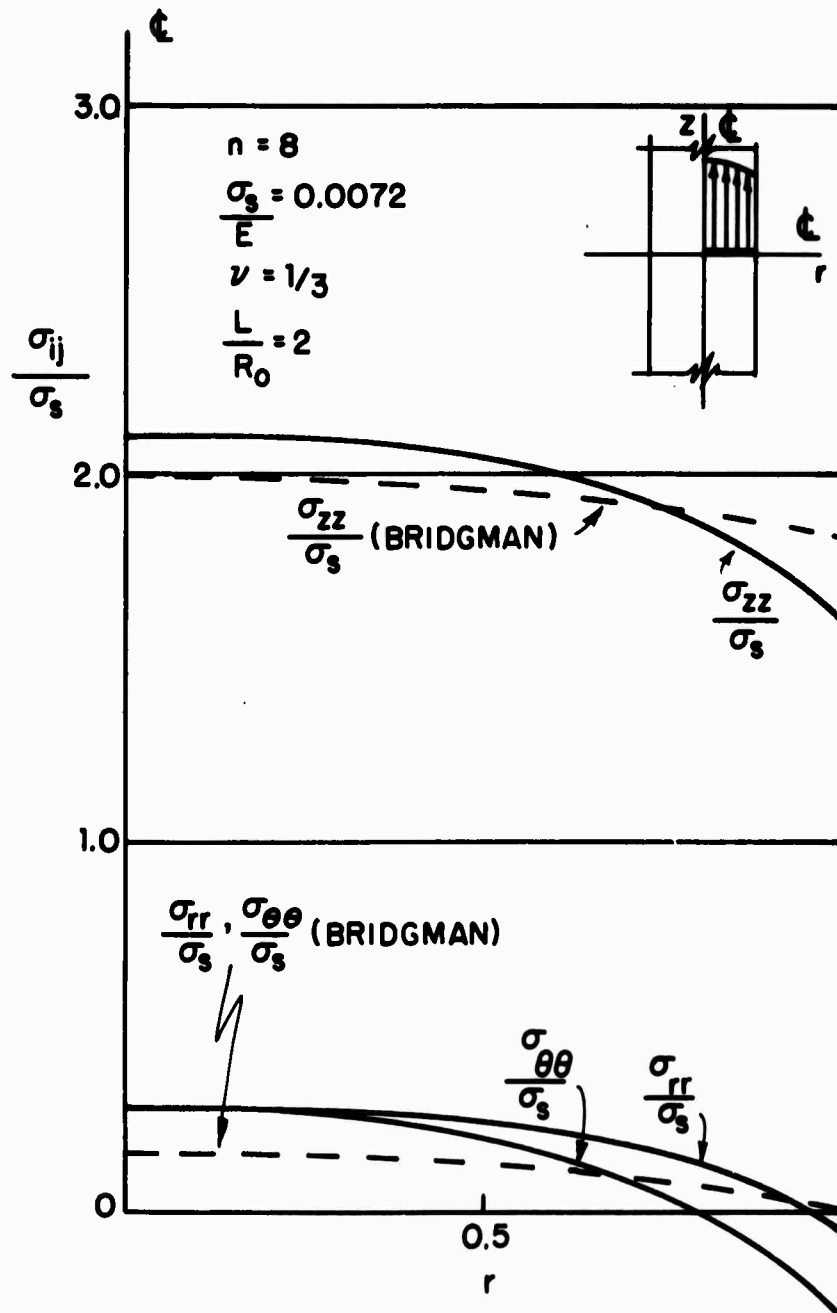AT THE NECK FOR $\frac{U_L}{L} = .35$

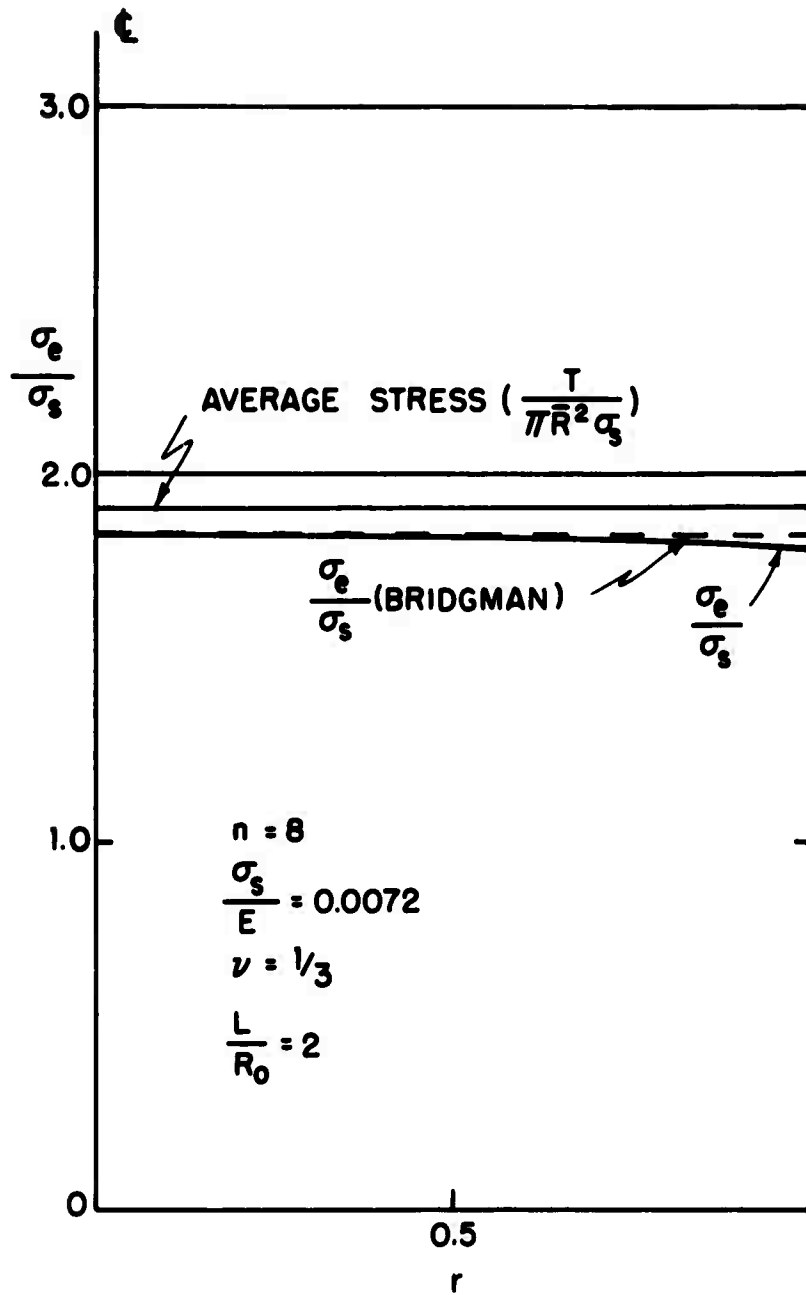FIG. 18A STRESS DISTRIBUTIONS AT THE NECK FOR $\frac{U_L}{L} = .25$

FIG. 18B EFFECTIVE STRESS DISTRIBUTION
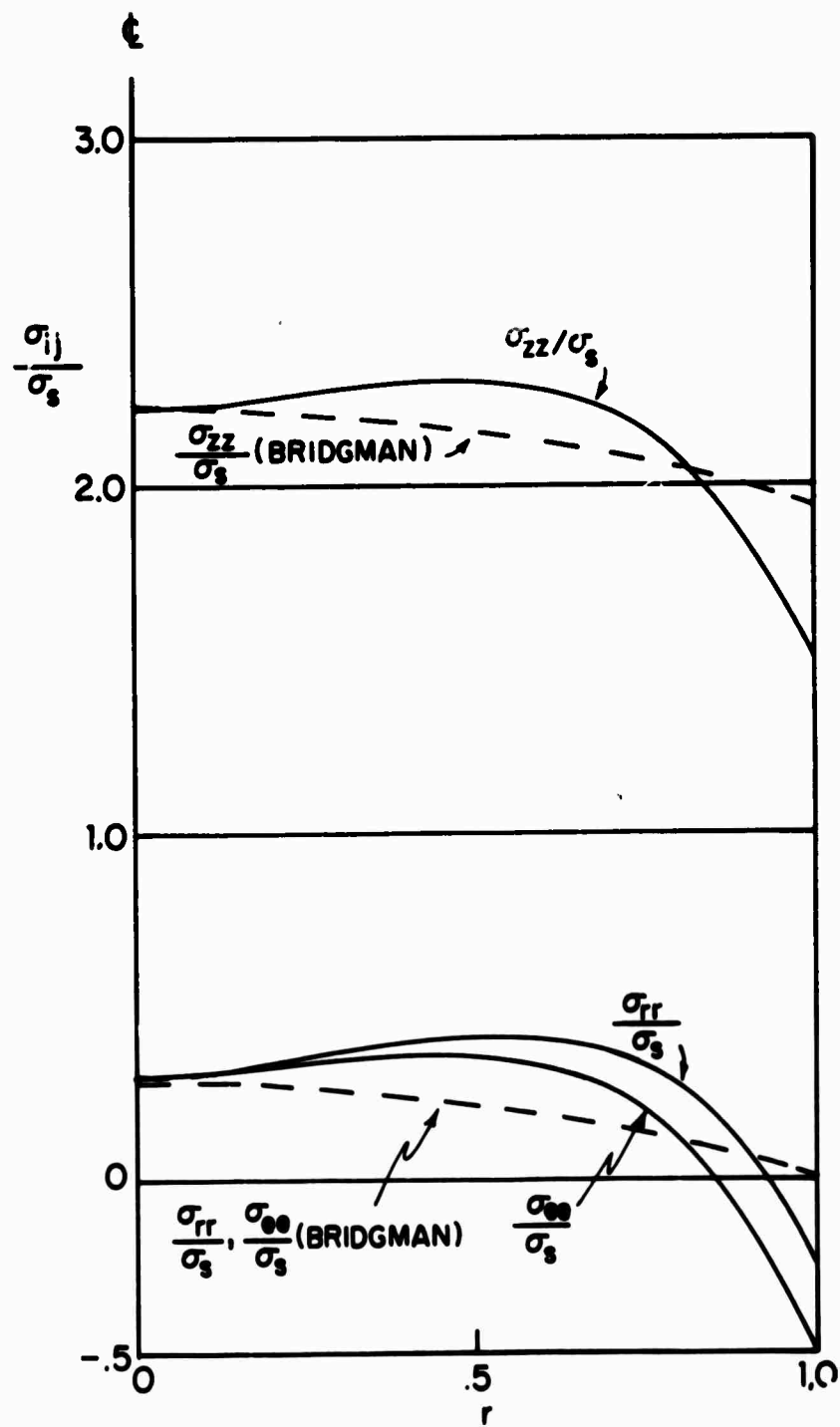AT THE NECK FOR $\frac{U_L}{L} = .25$

FIG. 19a STRESS DISTRIBUTIONS AT THE NECK FOR $\frac{U_L}{L}$ = .30
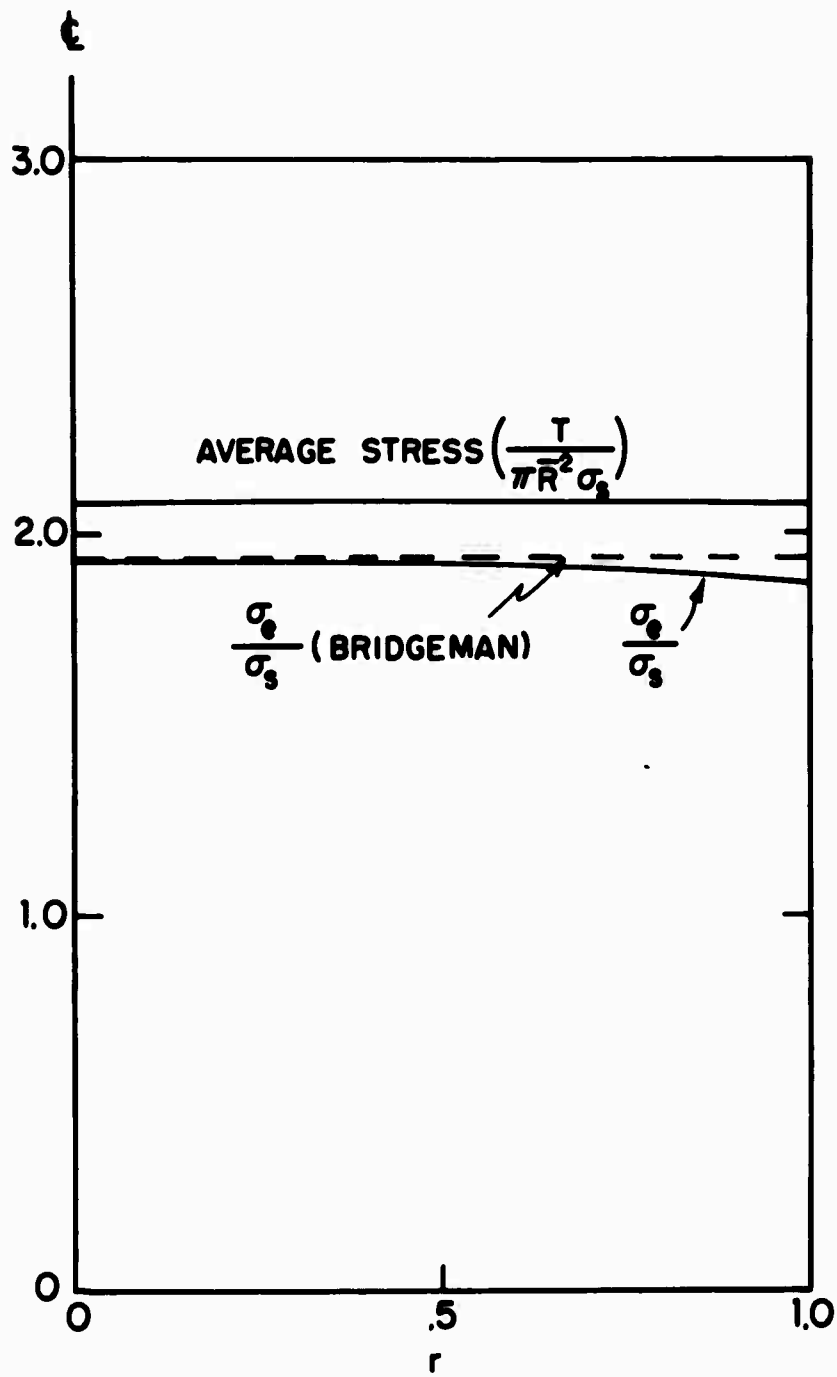
FIG. 19B EFFECTIVE STRESS DISTRIBUTION AT THE NECK FOR $\frac{U_L}{L} = .30$
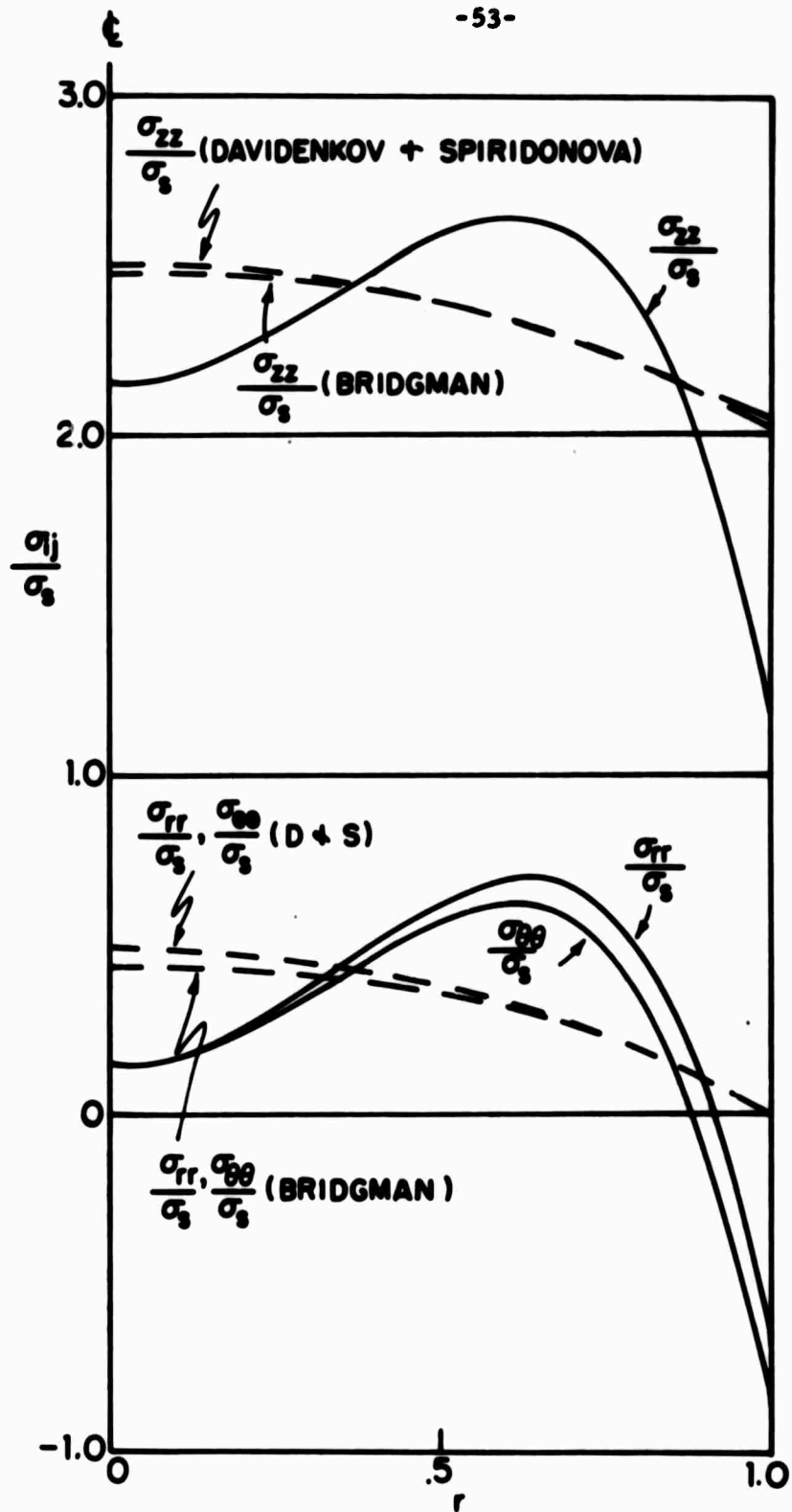
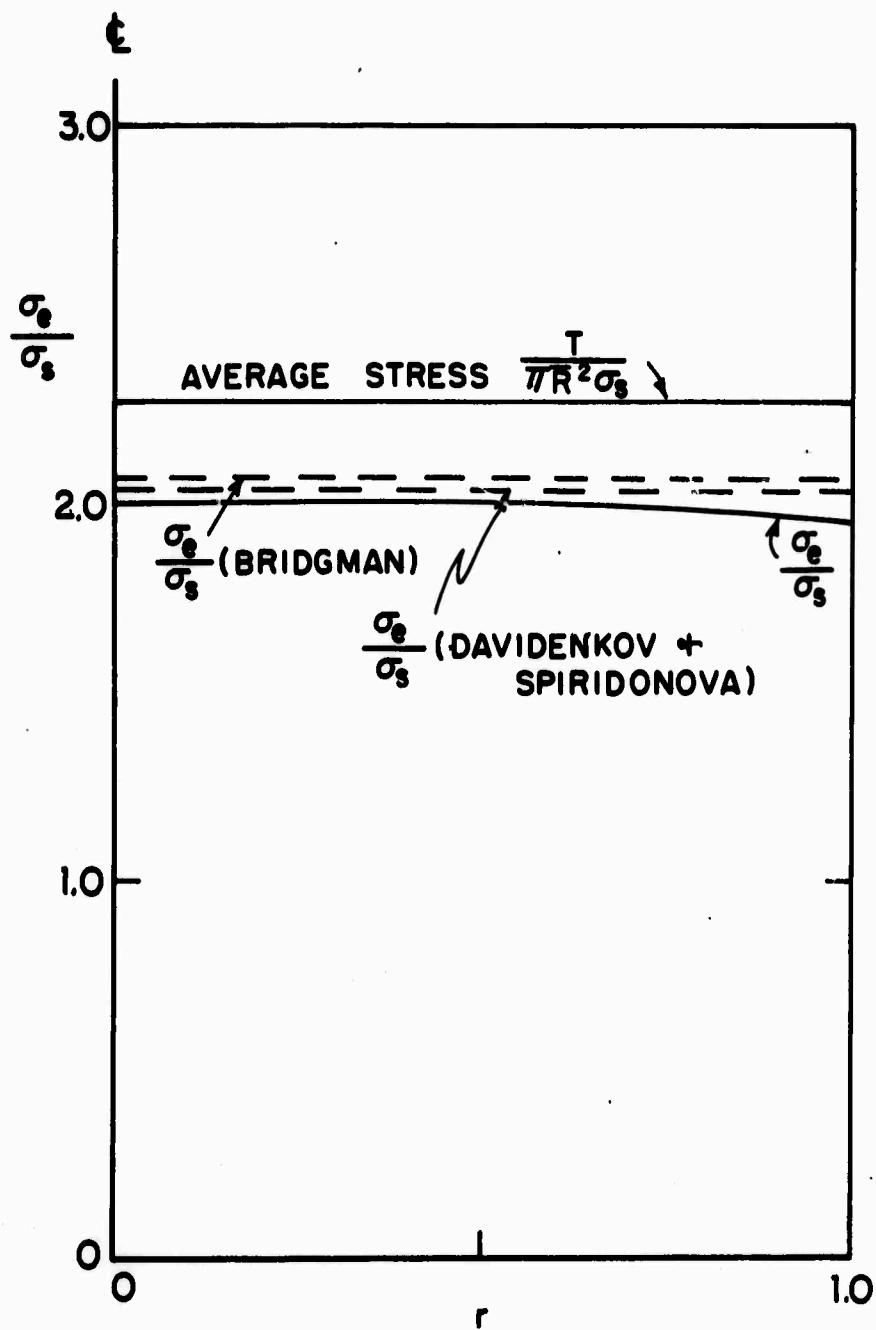FIG. 20A STRESS DISTRIBUTIONS AT THE NECK
FOR $\frac{U_L}{L} = .35$

FIG. 20B EFFECTIVE STRESS DISTRIBUTION AT THE NECK FOR $\frac{U_L}{L} = .35$

terms in the power expansions in r in the assumed displacements (34) and (35).) The results of the present analysis show that σ_{rr} becomes negative on the peripheral surface. However, these negative values for σ_{rr} are localized near the peripheral surface only. Therefore the stress distributions obtained may not be too incorrect inside the necked section. At $\dfrac{U_L}{L} = .50$, the negative value of σ_{rr} on the surface becomes about half of $(\sigma_{zz})_{max}$, and for this reason the calculation was terminated.

Also shown in Figs. 18, 19 and 20 are the stress distributions calculated by the formulas of Bridgman, and Davidenkov and Spiridonova, on the basis of the neck shapes predicted by the present analysis. These stress distributions are given by the formulas

(1) Bridgman

$$\frac{\sigma_e}{\sigma_s} = \frac{T}{\pi\sigma_s(\overline{R}^2 + 2\overline{R}\rho)\ln(1 + \frac{1}{2}\frac{\overline{R}}{\rho})}$$

$$\frac{\sigma_{rr}}{\sigma_s} = \frac{\sigma_{\theta\theta}}{\sigma_s} = (\frac{\sigma_e}{\sigma_s})\ln\frac{\overline{R}^2 + 2\overline{R}\rho - r^2}{2\overline{R}\rho}$$

$$\frac{\sigma_{zz}}{\sigma_s} = \frac{\sigma_e}{\sigma_s} + \frac{\sigma_{rr}}{\sigma_s}$$

(2) Davidenkov and Spiridonova

$$\frac{\sigma_e}{\sigma_s} = \frac{T}{\pi\sigma_s\overline{R}^2(1 + \frac{\overline{R}^2}{4\rho})}$$

$$\frac{\sigma_{rr}}{\sigma_s} = \frac{\sigma_{\theta\theta}}{\sigma_s} = (\frac{\sigma_e}{\sigma_s})\frac{(\overline{R}^2 - r^2)}{2\overline{R}\rho}$$

$$\frac{\sigma_{zz}}{\sigma_s} = \frac{\sigma_e}{\sigma_s} + \frac{\sigma_{rr}}{\sigma_s} \quad .$$

Here the total load T is calculated by (44), r is the distance from the center, $\bar{R}$ is the current neck radius, and ρ is the radius of curvature at the neck. Both $\bar{R}$ and ρ were measured from the calculated shapes of the tension specimen shown in Fig. 13. The effective stress calculated by [1] and [2] are seen to be close to the effective stress calculated by the present analysis. But this seems to be a coincidence since the detailed stress and strain distributions of the present analysis were not close to those of [1] and [2]. Perhaps it should be emphasized here that the above comparison may not be too meaningful, since the radius $\bar{R}$ and the radius of curvature ρ at the neck which were required for the calculation of the stress distributions given by Refs. [1] and [2], were provided by the present analysis.

VII. Concluding Remarks

The most significant result of the present analysis is that, for the first time, the shapes and the deformations of a necked-down tension specimen were rationally calculated. The stress and strain distributions in the specimen during its loading history were also found, although the numerical results for them are still far from conclusive.

Some improvements of the numerical technique will be needed for the present analysis to obtain more accurate results. Then, on the basis of the present analysis, the stress and the deformation of a tension specimen throughout its loading history can be predicted if the elastic constants and the strain-hardening characteristics of a material are known. This will provide knowledge of the stress conditions in a necked-down tension specimen before it fractures; thus it perhaps will lead to a better understanding of the fracture phenomena in a tension bar, such as the cup-cone type fracture.

APPENDIX

Inversion of the Constitutive Equation

Since

$$G_{ik}\dot{\sigma}^k_j = G_{ik}\frac{d}{dt}(\sigma^{kl}G_{jl})$$

$$= G_{ik}G_{jl}\dot{\sigma}^{kl} + 2G_{ik}\sigma^{kl}\dot{\eta}_{jl} \quad,$$

and

$$G_{jk}\dot{\sigma}^k_i = G_{jk}\frac{d}{dt}(\sigma^{kl}G_{il})$$

$$= G_{jk}G_{il}\dot{\sigma}^{kl} + 2G_{jk}\sigma^{kl}\dot{\eta}_{i)} \quad,$$

equation (10)a can be rewritten as

$$\dot{\eta}_{ij} = \frac{1}{E}\left[(1 + \nu)(\dot{\sigma}^{kl}G_{ik}G_{jl} + \sigma^{kl}G_{ik}\dot{\eta}_{jl} + \sigma^{kl}G_{jk}\dot{\eta}_{il}) - \nu G_{ij}\dot{\sigma}^k_k\right]$$

$$+ \frac{3}{2}(\frac{1}{E_t} - \frac{1}{E})(\sigma^{kl}G_{ik}G_{jl} - \frac{1}{3}G_{ij}\sigma^{kl}G_{kl})\frac{\dot{\sigma}_e}{\sigma_e} \quad. \tag{45}$$

We multiply both sides of (45) by $G^{ri}G^{sj}$ and rearrange it to get

$$\dot{\sigma}^{rs} = \frac{E}{(1 + \nu)}\left\{G^{ri}G^{sj}\dot{\eta}_{ij} - \frac{3}{2}(\frac{1}{E_t} - \frac{1}{E})(\sigma^{rs} - \frac{1}{3}G^{rs}\sigma^{kl}G_{kl})\frac{\dot{\sigma}_e}{\sigma_e}\right\}$$

$$+ \frac{\nu}{1 + \nu}G^{rs}\dot{\sigma}^k_k - (\sigma^{ri}G^{sj}\dot{\eta}_{ij} + \sigma^{si}G^{rj}\dot{\eta}_{ij}) \quad. \tag{46}$$

On the right hand side $\dot{\sigma}_e$ and $\dot{\sigma}^k_k$ are unknowns. In order to find $\dot{\sigma}^k_k$, we multiply (45) by G^{ij} to get

$$G^{ij}\dot{\eta}_{ij} = \frac{1}{E}\left[(1 + \nu)(\dot{\sigma}^{kl}G_{kl} + 2\sigma^{kl}\dot{\eta}_{kl}) - 3\nu\dot{\sigma}^k_k\right] \tag{47}$$

in which $(\dot{\sigma}^{kl}G_{kl} + 2\sigma^{kl}\dot{\eta}_{kl}) = \frac{d}{dt}(\sigma^{kl}G_{kl}) = \dot{\sigma}^k_k$. Rearranging (47) gives

$$\dot\sigma_k^k = \frac{E}{1 - 2\nu}\, G^{ij}\dot\eta_{ij} \qquad . \tag{48}$$

Next, in order to find $\dot\sigma_e$, we multiply (10)a by s^{ij} and obtain

$$s^{ij}\dot\eta_{ij} = \frac{1}{E}\left[(1 + \nu)s_j^i\dot\sigma_i^j\right] + \frac{3}{2}(\frac{1}{E_t} - \frac{1}{E})(s_j^i\sigma_i^j)\frac{\dot\sigma_e}{\sigma_e} \qquad . \tag{49}$$

With the use of the relations $s_j^i = \sigma_j^i - \frac{1}{3}\delta_j^i\sigma_k^k$, $\dot s_j^i = \dot\sigma_j^i - \frac{1}{3}\delta_j^i\dot\sigma_k^k$ and $\dot\sigma_e = \frac{3}{2}\frac{1}{\sigma_e}s_j^i\dot s_i^j$, equation (49) becomes

$$s^{ij}\dot\eta_{ij} = \{\frac{2}{3}\frac{1 + \nu}{E} + (\frac{1}{E_t} - \frac{1}{E})\}\sigma_e\dot\sigma_e$$

whence

$$\dot\sigma_e = \frac{1}{\sigma_e}\left\{\frac{s^{ij}\dot\eta_{ij}}{\frac{2}{3}\frac{1 + \nu}{E} + (\frac{1}{E_t} - \frac{1}{E})}\right\} \tag{50}$$

Note that in (50), $(\frac{1}{E_t} - \frac{1}{E})$ is always positive, so that the loading condition $\dot\sigma_e \geq 0$ can be replaced by $s^{ij}\dot\eta_{ij} \geq 0$. Substitution of (48) and (50) into (46) gives the final form of the inverted constitutive relations

$$\left\{\begin{array}{l}\dot\sigma^{ij} = \frac{E}{(1 + \nu)}\left\{G^{ik}G^{jl}\dot\eta_{kl} - \frac{3}{2}\frac{s^{ij}(\frac{1}{E_t} - \frac{1}{E})s^{kl}\dot\eta_{kl}}{\sigma_e^2(\frac{2}{3}\frac{(1 + \nu)}{E} + (\frac{1}{E_t} - \frac{1}{E}))}\right\}\\[6mm]\qquad + \frac{\nu E}{(1 + \nu)(1 - 2\nu)}G^{ij}G^{kl}\dot\eta_{kl} - (\sigma^{ik}G^{jl}\dot\eta_{kl} + \sigma^{jk}G^{il}\dot\eta_{kl})\\[4mm]\qquad\qquad\qquad\quad\text{if } \sigma_e = c \text{ and } s^{ij}\dot\eta_{ij} \geq 0\\[6mm]\dot\sigma^{ij} = \frac{E}{(1 + \nu)}G^{ik}G^{jl}\dot\eta_{kl} + \frac{\nu E}{(1 + \nu)(1 - 2\nu)}G^{ij}G^{kl}\dot\eta_{kl}\\[4mm]\qquad - (\sigma^{ik}G^{jl}\dot\eta_{kl} + \sigma^{jk}G^{il}\dot\eta_{kl}) \qquad\text{if } \sigma_e < c,\\[4mm]\qquad\qquad\qquad\quad\text{or } \sigma_e = c \text{ and } s^{ij}\dot\eta_{ij} \leq 0 \qquad .\end{array}\right.$$

REFERENCES

1. Bridgman, P. W., "Studies in Large Plastic Flow and Fracture, " Harvard University Press, Cambridge, 1964, Chapter 1.

2. Davidenkov, N. N., and Spiridonova, N. I., "Mechanical Method of Testing Analysis of the State of Stress in the Neck of a Tension Test Specimen, " Proceedings of American Society for Testing Materials, Volume 46, 1946, pp. 1147.

3. Thomason, P. F., "An Analysis of Necking in Axi-Symmetric Tension Specimens, " International Journal of Mechanical Sciences, " Volume 11, 1969, pp. 481.

4. Segal, V. M., "Plastic Flow During the Necking of Axisymmetric Samples Under Tension, " Zhurnal Prikladnoi Mekhaniki i Tekhnicheskoi Fiziki, March-April, 1969, pp. 141-147, in Russian.

5. Kantorovich, L. V., and Krylov, V. I., "Approximate Methods of Higher Analysis, " Interscience Publishers, Inc., New York, 1964.

6. Budiansky, B., "Remarks on Theories of Solid and Structural Mechanics, " Problems of Hydrodynamics and Continuum Mechanics, Society for Industrial and Applied Mathematics, Philadelphia, 1969, pp. 77.

7. Green, A. E., and Naghdi, P. M., "A General Theory of an Elastic-Plastic Continuum, " Archive for Rational Mechanics and Analysis, Volume 18, pp. 251.

8. Lee, E. H., and Liu, D. T., "Finite Strain Elastic-Plastic Theory, " Proceedings, IUTAM Symposium of Irreversible Aspects of Continuum Mechanics, Springer Verlag, Vienna, 1968, pp. 213.

9. Cameron, I. G., and Scorgie, G. C., "Dynamics of Intense Underground Explosions, " Journal of the Institute of Mathematics and Its Applications, Volume 4, Number 2, June 1968, pp. 194.

10. Lee, E. H., "Elastic-Plastic Deformation at Finite Strains, " Journal of Applied Mechanics, Volume 36, Number 1, March 1969, pp. 1.

11. Willis, J. R., "Some Constitutive Equations Applicable to Problems of Large Dynamic Plastic Deformation, " Journal of the Mechanics and Physics of Solids, Volume 17, Number 5, October 1969, pp. 359.

12. Budiansky, B., Through Private Communication.

13. Ramberg, W., and Osgood, W. R., "Description of Stress-Strain Curves by Three Parameters, " National Advisory Committee for Aeronautics, Technical Note Number 902.

14. Budiansky, B., and Radkowski, P. P., "Numerical Analysis of Unsymmetrical Bending of Shells of Revolution, " AIAA Journal, Volume 1, Number 8, August 1963, pp. 1833.

DOCUMENT CONTROL DATA · R & D

Security classification of title, body of abstract and indexing annotation must be entered when the overall report is classified

1. ORIGINATING ACTIVITY (Corporate author)	2a. REPORT SECURITY CLASSIFICATION
Division of Engineering and Applied Physics Harvard University Cambridge, Mass. 02138	Unclassified
	2b. GROUP

3. REPORT TITLE

NECKING IN A BAR

4. DESCRIPTIVE NOTES (Type of report and inclusive dates)

Interim technical report

5. AUTHOR(S) (First name, middle initial, last name)

Winston H. Chen

6. REPORT DATE	7a. TOTAL NO. OF PAGES	7b. NO. OF REFS
March 1970	67	14

8a. CONTRACT OR GRANT NO.	9a. ORIGINATOR'S REPORT NUMBER(S)
ARPA SD-88	
b. PROJECT NO.	Technical Report No. ARPA-40
c.	9b. OTHER REPORT NO(S) (Any other numbers that may be assigned this report)
d.	

10. DISTRIBUTION STATEMENT

Reproduction in whole or in part is permitted by the U. S. Government. Distribution of this document is unlimited.

11. SUPPLEMENTARY NOTES	12. SPONSORING MILITARY ACTIVITY

13. ABSTRACT

The necking process of an axisymmetric tension specimen made of elastic-plastic, strain-hardening material is analyzed by a generalized J_2-flow theory for large deformations. The governing equations are solved in a Kantorovich type approach based on a variational principle. The effects of both geometric nonlinearities resulting from large deformations and the physical nonlinearities arising from plastic material behavior are considered. Numerical results have been found for the stress and deformation histories in the specimen up to a 50% reduction of the neck radius. The shape of the neck, for the first time, is rationally calculated.

DD FORM 1473 (PAGE 1)

KEY WORDS	LINK A		LINK B		LINK C	
	ROLE	WT	ROLE	WT	ROLE	WT
Solid Mechanics						
Axisymmetric Tension Test						
Necking						
Plastic Flow						
Strain-Hardening						

DD FORM 1473 (BACK)

1 NOV 65

S/N 0101-807-6821